Ref. Ares(2024)2552800 - 08/04/2024

Better Contrails Mitigation - BeCoM

D1.1

Upgraded instrumentation and Lidar inversion software

Delivery Date:	30/11/2023 (M18)
Date of submission:	08/04/2024

LEAD BENEFICIARY FOR THIS DELIVERABLE			
Name:	CNRS		
Contact Person:	Philippe Keckhut		
E-mail:	Keckhut@latmos.ipsl.fr		
AUTHORS			
Participants:	CNRS		
Work Package:	WP 1		
Version:	1	Number of Pages:	

REVISION HISTORY			
VERSION	DATE	AUTHOR / REVIEWER	NOTES
1	27/08/2023	Philippe Keckhut	Section 2
2	13/12/2023	Sidy Diara	Section 4
3	21/03/2024	Dunya Alraddawi	Section 3

REVIEWED AND SIGNED OFF BY			
ROLE	DATE	NAME	SIGNATURE
WP3 Lead	08/04/2024	Teodora Petrisor	

This project has received funding from the European Union's Horizon Europe Research and innovation program under Grant Agreement No 101056885

List of abbreviations

COPDD	Cézeaux Opme Puy De Dôme
EARLINET	European Aerosol Research Lidar Network
ECMWF	European Centre for Medium-range Weather Forecasts
GRUAN	GCOS Reference Upper-Air Network
IPRAL	*IPSL* Hi-Performance multi-wavelength Raman *Lidar*
NDACC	Network for Detection of Atmospheric Composition Changes
OHP	Observatory of Haute-Provence
OPAR	*Observatoire* de Physique de l'Atmosphère de La Réunion
SNR	Signal to Noise Ratio
CFH	Cryogenic Frost Point Hygrometer
GNSS	Global Navigation Satellite System
IWV	Integrated Water Vapor
FTIR	Fourrier Transform Infrared Spectroscopy

This project has received funding from the European Union's Horizon Europe
Research and innovation program under Grant Agreement No 101056885

List of figures

List of tables

This project has received funding from the European Union's Horizon Europe Research and innovation program under Grant Agreement No 101056885

Abstract

This deliverable aims to describe the ground observations put into service within the framework of the BECOM project. The objective is to be able to have reliable data to evaluate the water vapor content which is one of the main uncertainties to better understand the conditions of contrail formation. Current observations are marred by high uncertainties and make it difficult to estimate the super-saturation necessary for the formation of clouds and more specifically contrails.

The most innovative device is based on existing water vapor Raman lidars which make it possible to provide water vapor concentration profiles up to the upper troposphere where contrails are formed. The great advantage and originality of these data is their perfect simultaneity with the detection of contrails. During the first phase of the project these instruments were reactivated in order to provide regular data. Meetings between the teams from the different sites were organized. Some, like the lidar at the Haute-Provence Observatory, have even been improved in order to have observations starting from the ground. This document describes these systems, their characteristics and their performances.

One of the challenges of measuring water vapor by Raman lidar is to have a common analysis method, particularly for calibration. Until now, several methods had been proposed and applied to lidars. The calibration method is based on meteorological analysis data from the European ERA5 center due to their wide availability. This document describes the calibration method, its limits and the associated uncertainties.

Radiosounds being another source of relevant data launched close to lidar sites, the latter are analyzed and, although not available in perfect coincidence with the appearance of contrails, compared with the ERA5 analysis. Biases appear and a first correction method is proposed to reconcile ERA5 and radiosonde observations in the cruise altitude associated with air traffic.

The current report describes the French Raman lidar systems and upgrades in addition to a united lidar software of the 4 lidar systems together with uncertainty assessment of nearby used datasets.

This project has received funding from the European Union's Horizon Europe Research and innovation program under Grant Agreement No 101056885

Table of content

This project has received funding from the European Union's Horizon Europe Research and innovation program under Grant Agreement No 101056885

This project has received funding from the European Union's Horizon Europe
Research and innovation program under Grant Agreement No 101056885

1. Introduction

Lidar methods offers a unique advantage of obtaining simultaneous and collocated Water Vapor vertical profiling (WVMR) retrieved from backscattered lidar signals. This technique also enables the characterization of cloud vertical location and structure as they pass over the measurement site, allowing for continuous monitoring of atmospheric humidity, especially before and after contrail transit, though it may be limited by the presence of low clouds.

The Raman method offers easier implementation and achieves the necessary vertical range for contrail analysis by inducing a wavelength shift through the Raman effect.

Despite its capabilities, lidar water vapor measurements face limitations. Hardware challenges of removing the elastic scattering and ensuring sufficient signal strength to reach the tropopause, where contrails form. Additionally, lidar measurements are susceptible to atmospheric conditions, including the presence of low clouds, which can impact their effectiveness.

Lidar-based water vapor measurements are particularly sensitive to atmospheric conditions variability with altitude. Hence, a careful calibration is needed. The Calibration efforts often rely on collocated external measurements, such as radiosondes, CFH sondes, and models, to ensure accuracy and reliability, and more importantly to achieve a unified calibration strategy across multiple lidar sites.

The integration of radiosonde data from M10 sites, co-located with lidar installations, has enabled the evaluation of lidar humidity levels and those simulated by meteorological forecasts from the European Centre for Medium-Range Weather Forecasts (ECMWF) via the ERA5 analysis product, enhancing our understanding of atmospheric moisture dynamics and improving forecast accuracy.

Addressing these challenges is essential for advancing our understanding of atmospheric dynamics and improving the accuracy of lidar-based water vapor measurements.

The primary objective of this Deliverable is to ensure the readiness and optimal functioning of the four Raman lidars involved in this project, facilitating the implementation of final hardware lidar systems for improved measurements. Section 2 will describe the four French lidar systems involved in this project: challenges and upgrades, Section 3 will describe the treatment channel of water vapor profiles and the calibration strategy to be applied on all sites, Section 4 evaluate the uncertainty and limitations of available supported referenced datasets to be used in the calibration & validation (at this stage radiosondes and model). Subsequent milestones will focus on data analysis, including calibration and validation campaigns to enhance accuracy estimates.

2. Lidar instrumentation for systematic operation consolidated

2.1. Introduction

Water vapor vertical profile can be provided by lidar methods. The main advantage of this method is the possibility to have vertical profiles simultaneously and collocated with backscattered lidar. Backscattered lidar can provide the vertical location and shape of clouds when they pass at the vertical of the site. Continuous operations can provide the atmospheric humidity before and after the contrail has transited over the lidar beam. The main limitation is due to presence of low clouds.

Water vapor can be obtained with lidar method in using two techniques: the dial and the Raman methods. The first one requires to have two lasers with wavelength absorbed and non-absorbed by the target component. While this technique is more complex to implement a vertical range up to the upper troposphere (where contrails can be found) is more complex to achieve, as one beam is absorbed and then quickly in-operant. The second method is easier to implement as it requires only

This project has received funding from the European Union's Horizon Europe
Research and innovation program under Grant Agreement No 101056885

one laser that can be similar with the one used for the backscattered channel. Raman effect induces a wavelength shift and then the photon collection is performed in a distinct spectral band.

The hardware challenges consist in fully removing elastic scattering (rejection) and having enough signal to reach the tropopause where contrails are formed. The method faces some issues of calibration.

The objective of this delivrable consists in insuring that the 4 Raman lidars involved in this project will be ready to operate and final hardware lidar systems will be implemented for providing the best measurements.

Section (3) will be dedicated to the data analyses and will include calibration strategy while a validation campaign is planned and will be detailed in a next deliverable to provide accuracy estimates.

2.2. The past situation and challenges

One of the difficulties with Raman lidar is the weak signal requiring powerful lidar and large collector to reach the upper troposphere. Many systems are limited to lower altitude investigations. The water vapor profile was defined as one target component of the NDACC (Network for Detection of Atmospheric Composition Changes). The NDACC lidar group selects Raman method for water vapor and exchanges experiences between groups to achieve such a challenge.

Raman measurements are performed with the ratio of the Raman water vapor channel and the Nitrogen Raman Channel. Then a direct measurement of the water vapor mixing ratio is obtained.

H_2O Raman Lidar: q(z) H_2O mixing ratio is specified as:

$$\underbrace{q(z)}_{\text{Mass } H_2O\ /\ \text{Dry air mass}}=\frac{n_{H_2O}(z)}{n_{N_2}(z)}\times\underbrace{\left(\frac{M_{H_2O}}{M_{N_2}}\times r_{N_2}\right)}_{k}=\underbrace{\frac{N_{H_2O}}{N_{N_2}}}_{\text{Lidar Raman signal for nitrogen \& water vapor}}\underbrace{\frac{T_a(\lambda_{Ram_{N_2}},z)}{T_a(\lambda_{Ram_{H_2O}},z)}}_{\text{Atmospheric transmission at } \lambda_{Ram}}\frac{\overbrace{K_{N_2}}^{\text{Calibration constant}}}{K_{H_2O}}\underbrace{\frac{\sigma_{N_2}}{\sigma_{H_2O}}}_{\text{Differential Raman backscattering cross sections for water vapor \& nitrogen}}k$$

2

The main challenge of the water vapor Raman signal is related to the weak signal that is 9 magnitudes smaller than Rayleigh scattering and 2-3 more magnitudes with elastic scattering from clouds. Lidar systems need to use powerful laser and large telescope area (see table 1). Also, the main bias can come from the elastic signal rejection (12 magnitudes) to have water vapor profile insensitive to molecular and mainly cloud effects. First experiences also show that large elastic scattering can induce fluorescence effects on optical devices. Careful choice of optical devices must be performed mainly with optical fibers. Optical fibers were efficient to collect the signal, however because of this induced effect, they were avoided on the new systems or elastic signal removed before entering the water vapor lidar system.

Another important issue is the calibration (Vérèmes et al., 2019). This is usually ensured by comparing lidar observations with balloon observations in the lower altitude ranges where balloon sondes exhibit their best accuracies. This method presents some uncertainties due to the non-perfect alignment between balloon profile and lidar profile due to the drifting of the balloon. More sophisticated techniques are using calibration with total water vapor column measured with independent method, but they requires coaxial lidar configuration to reach the ground. The issue of calibration will be investigated later in section 3.

This project has received funding from the European Union's Horizon Europe Research and innovation program under Grant Agreement No 101056885

CNRS' research lidars for monitoring are going to be renewed and will be rebuilt following a standard that is going to be defined. The main objective consists to operate the lidars automatically. This new system will be not operational for this project.

2.3. Lidar description

2.3.1. Main Lidar Characteristics

The two main important characteristics for the Raman lidar providing water vapor in the upper troposphere simultaneously with backscattering profiles, are the lidar power (product of collector area and lidar power) to obtain a significant measurement and the rejection capability that is required to separate Raman to the much more intense elastic scattering. In this project, CNRS has developed 4 Raman lidars including 2 NDACC systems, one relatively powerful lidar but not affiliated to NDACC and a system dedicated for lower altitudes. These different systems are involved in BeCom project allowing to have a better view of their potential contributions in contrail investigations for future operational deployment. About rejection, the four lidar have been developed by LATMOS/ CNRS laboratory and its Spin-off company called Gordien-Strato. Similar rejection efficiency has been implemented in the four systems. It has been demonstrated that the elastic signal is fully removed and water vapor profile non-affected by such effect. Preliminary experiences have also shown that fluorescence effect can occur on optical fibers. Most of the recent systems were designed without optical fibers.

About the Lidar Power, the different characteristics are provided in table 1.

- OPAR system installed in tropical region is the more recent and more sophisticated system. This lidar is dedicated to the transport through UTLS zone (Upper Troposphere and Lower Stratosphere). The location is not the best for contrail investigation. However, for the validation of the global meteorological analyses and satellite observations, this system is well adapted.
- The OHP located in south of France (Manosque) is also quite powerful and will be the best system for contrail investigations. However, its design needs to be improved with a similar configuration to OPAR. Mainly the coaxial configuration will allow to remove optical fibers and insured better calibration in providing profiles from the ground.
- IPRAL system is also a recent instrument dedicated for aerosol investigations. A water vapor is included and for operational reason, it was not designed with a coaxial configuration.
- OPGC system is a lidar system also dedicated to aerosol investigations and is less powerful than the other ones. The main interest of this system will be to evaluate the potential contribution for contrail for such modest systems that can be deployed more easily for a reduced cost.

This project has received funding from the European Union's Horizon Europe Research and innovation program under Grant Agreement No 101056885

Lidar name	Location	Wavelength	Lidar Power J.m²	Emission configuration	Contacts
OPAR	La Réunion (20°S)	355 nm	12,7	Coaxial	Valentin Duflot Guillaume Payen
OHP	South of France (44°N)	532 nm	7,5	Biaxial	Philippe Keckhut
IPRAL	Vicinity of Paris (49°N)	355 nm	2,2	Biaxial	Jean-Charles Dupont Christophe Pietras
OPGC	Center of France (46°N)	355 nm	0,08	Biaxial	Jean-Luc Baray, Patrick Freville

Table 1. List of the Raman lidar deployed in the France territory

2.3.2. Description of the different lidars

2.3.2.1. IPRAL System

The IPRAL system is a multiwavelength lidar emitting at 355 and 532 nm with a Nd:Yag laser of 375 mJ/pulse. The 6 receiving channels include elastic, Nitrogen and Water Vapor channels and polarization channels. The telescope is a 500 m diameter. The system exhibits a SNR larger than 3 at 10-12 km altitude heights for a 20 minutes integration time. The system is equipped with 2 channels with two different sensitivities, field of view and valid altitude range providing a full overlapping and Raman signals down to the ground even if the configuration is non-coaxial. The system operates continuously with an automatic mode. This system is ready to operate for simultaneous water vapor and cloud measurements. At this time the aerosol mode was used but water vapor requires to improve signal analyses (objectives of Milestone 1.3). This system has a great value as regular well-calibrated radiosondes were launched within the GRUAN Network.

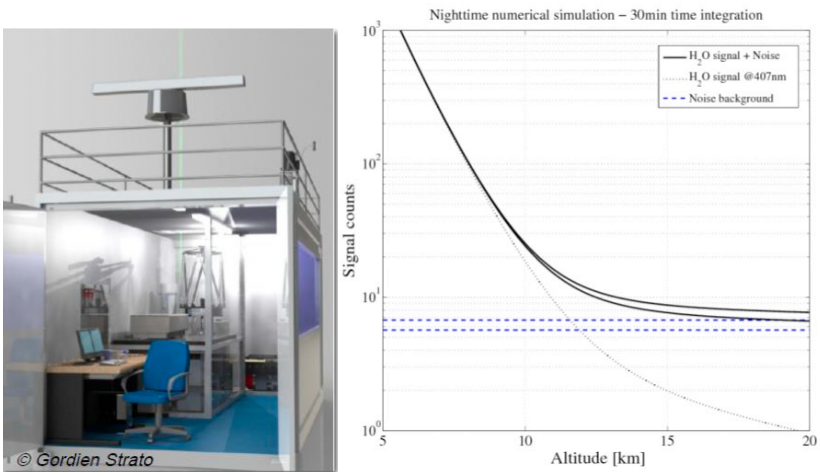

Figure 1. View of the IPRAL lidar and an example of lidar signals

This project has received funding from the European Union's Horizon Europe Research and innovation program under Grant Agreement No 101056885

2.3.2.2. OPGC System

The system installed at Puy de Dôme (Clermont-Ferrand, France), was designed by the same company as IPRAL with a ND:YAG laser emitting 60 mJ/pulse at 355 nm 4 receiving channels. This system is designed for aerosol and cloud analyses within EARLINET-ACTRIS framework (Baray et al. 2018). It includes 2 polarization channels and Nitrogen and Water Vapor Raman channels. The telescope diameter is 400 mm. The field of view of 0,25 mrad exhibits signals after 500 meters. While the system is non-coaxial, the calibration with total column is not directly possible and calibration is ensured with radiosondes. While this system is less powerful than the other lidars, it will be interesting to evaluate during the course of BeCoM the usefulness of such similar lidar system.

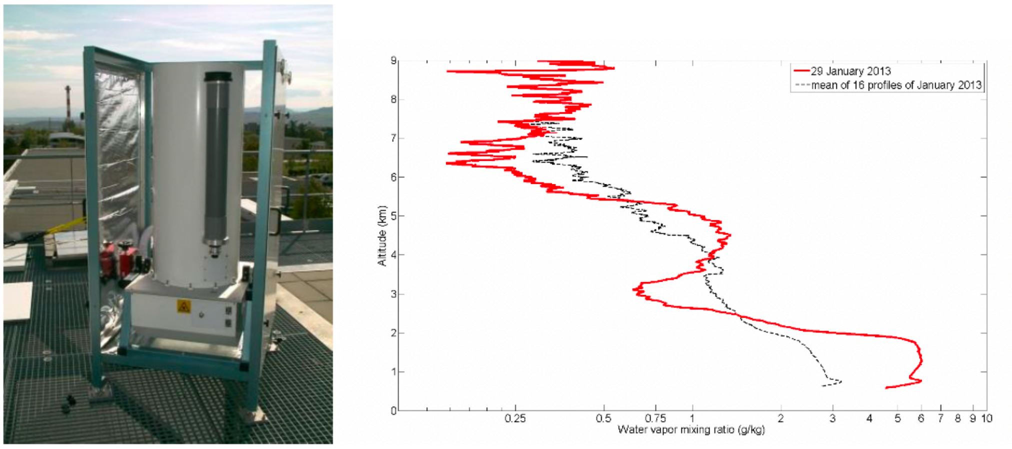

Figure 2. View of the COPDD L lidar and an example of water vapor profile obtained on January 2013 and compared with a mean profile calculated with radiosondes.

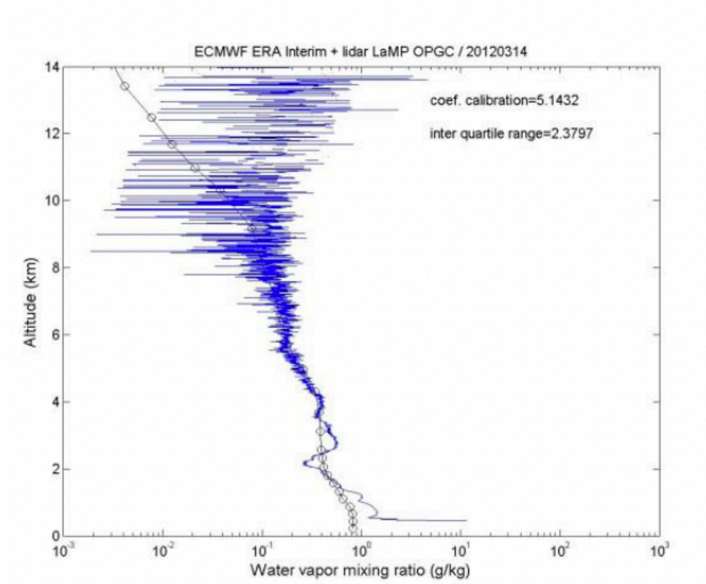

Figure 3. Water vapor profile obtained on Mars 14th, 2012 and calibrated wit ECMWF-ERA interim between 2 and 5 kilometers.

This project has received funding from the European Union's Horizon Europe Research and innovation program under Grant Agreement No 101056885

2.3.2.3. OPAR System

The OPAR system has been designed in the framework of the NDACC to investigate the transport of water vapor through the tropopause. This lidar system built by Gordien_Strato company takes advantage of all the preliminary designs performed in France by LATMOS (Hoareau et al., 2012). It is based on a coaxial configuration and includes no optical fibers. It is one of the most powerful lidars in the world with a telescope diameter of 1200 mm and a laser of 400 mJ/pulse at 355 nm (That can be doubled). This system is using 5 channels and was designed to include also 3 elastic channels for temperature and aerosol retrieval with molecular and particle scattering (Dionisi et al., 2015). While there are few contrails over the site, this accurate water vapor observations are useful to evaluate actual meteorological analyses.

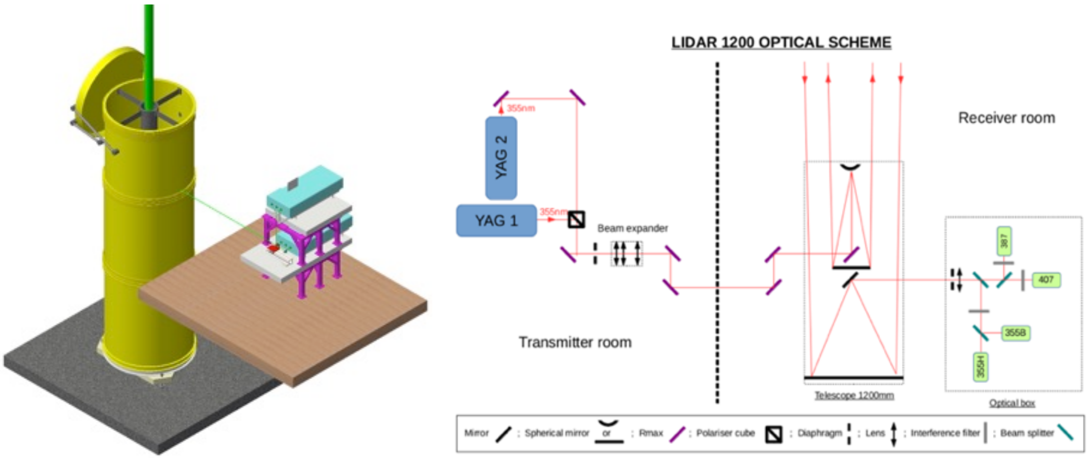

Figure 4. Optical scheme of the OPAR Lidar (Aerosol channel is obtained with an independent telescope and is not represented here.

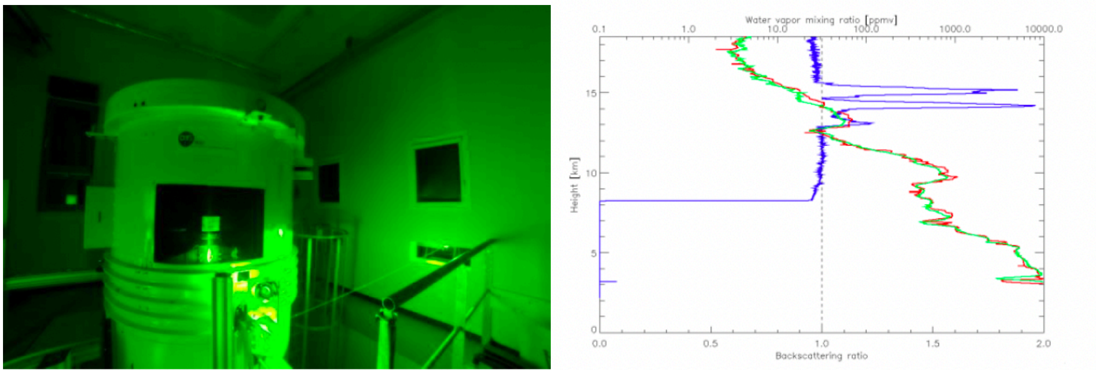

Figure 5. Water vapor lidar profile (Green) obtained on April 8th, simultaneously with backscattering profile (blue) exhibiting a cirrus cloud around 15 km. In red the water vapor derived from a collocated RS92 radiosonde is represented .

2.3.2.4. OHP System

The system installed at the Observatory of Haute Provence (OHP) is one of the first powerful water vapor lidar systems (1995). It was installed on an existing Rayleigh system designed for the temperature and the aerosol measurements starting in 1978 (sherlock et al., 1999). The water vapor channel is using a 800 mm telescope and a Nd:Yag laser of 300 mJ/pulse at 532 nm. The multi-channel system was designed with a mosaic of mirrors coupled with optical fibers. First water climatology with Raman lidar were performed (Hoareau et al., 2009) and calibration issues were addressed.

This project has received funding from the European Union’s Horizon Europe Research and innovation program under Grant Agreement No 101056885

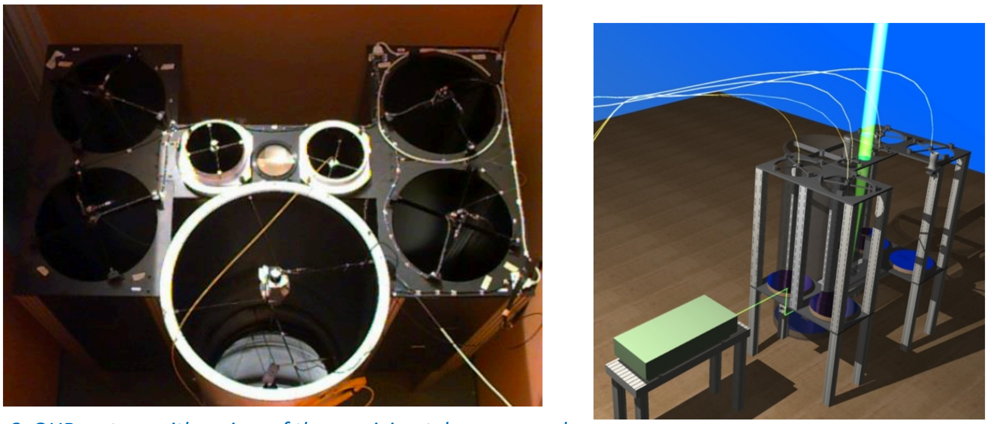

Figure 6. OHP system with a view of the receiving telescopes and the associated optical fiber system.

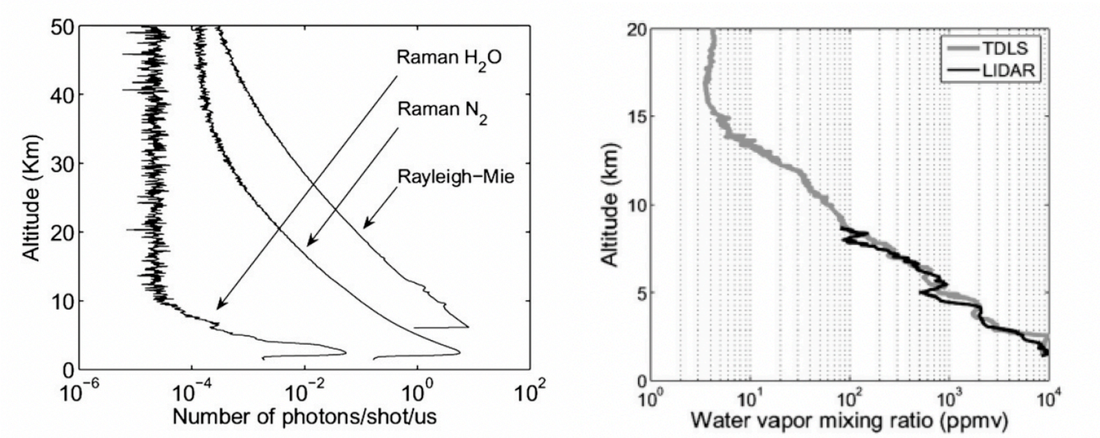

Figure 7. OHP lidar signals and an example of a water vapor profile compared with a balloon-board laser diode system dedicated for low density H2O measurements.

2.4. New implementations at OHP

To ensure a better calibration, it is necessary to collect lidar signal down to the ground like the OPAR implementation. The potential fluorescence effect by optical fiber requires to remove these devices and have a direct detection. It was proposed to modify the lidar design with a coaxial configuration. It was asked to Gordien_Strato that have already implemented a similar system at La Réunion to provide a proposal. The technical proposal and the quotation were submitted on February 1st 2023. The company was not able to implement the new system before July 2023 as planned initially because of security reasons. CNRS-INSU director and the head of the observatory of Haute-Provence have stopped operations and access to the lidar station for several months to implement legal security infrastructure that were missing. The hardware for the coaxial configuration was perfectly implemented. Lidar signals are not yet nominal. The setting will be performed in the coming weeks.

This project has received funding from the European Union's Horizon Europe Research and innovation program under Grant Agreement No 101056885

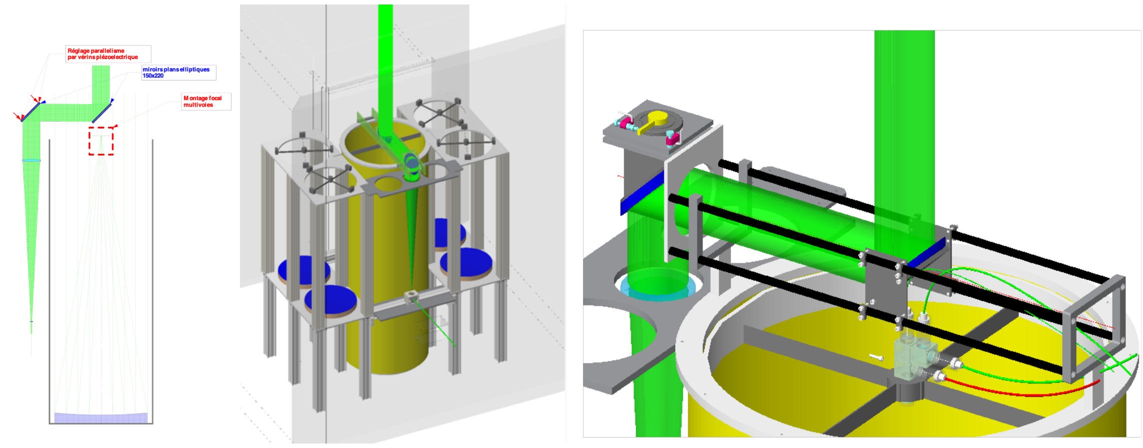

Figure 8. view of the new OHP lidar design with a stroboscope type of emission, in the middle the 4 Rayleigh mirrors are represented while the right panel show a zoom of this new emission system.

2.5. Conclusions

The 4 lidars involved in BeCoM will provide water vapor density profiles.

Main characteristics and references of the different lidars were provided. Their different roles in the project are the following:

- The most powerful one located at La Réunion (tropical zone) will be used to calibrate ECMWF and satellite observations while it provides accurate profiles up to the stratosphere.
- The lidar at OHP (south of France) will be the main instrument to have collocated accurate water vapor profiles and contrail altitudes. A major design evolution was made to improve calibration for future observations
- IPARL Lidar at Palaiseau (close to Paris) is a new system that should provide promising water vapor profiles with contrail detection. Water vapor has not been fully validated and software used on other sites needs to be adapted. The plus-value is performed by the regular balloon launches with well calibrated water vapor measurements performed within GRUAN.
- The lidar installed at Clermont-Ferrand observatory is a more modest system better adapted for lower-mid troposphere investigations but probably easier to involve on a potential future network dedicated to contrail monitoring.

2.6. References

Baray J.L. Fréville P., Montoux N., Hadad D., Sellegri K., A Lidar at Clermont-Ferrand-France to describe the boundary layer dynamics, aerosols, cirrus and tropospheric water vapor, Proceeding of the 28th ILRC conference, 2018.

Dionisi, D., Keckhut, P., Courcoux, Y., Hauchecorne, A., Porteneuve, J., Baray, J. L., Leclair de Bellevue, J., Vérèmes, H., Gabarrot, F., Payen, G., Decoupes, R., and Cammas, J. P., Water vapor observations up to the lower stratosphere through the Raman lidar during the Maïdo lidar calibration campaign, Atmos. Meas. Tech., 8, 1425-1445, doi:10.5194/amt-8-1425-2015, 2015.

This project has received funding from the European Union's Horizon Europe Research and innovation program under Grant Agreement No 101056885

Hoareau, C., P. Keckhut, A. Sarkissian, J-L. Baray, And G. Durry, Methodology for water monitoring in upper troposphere with Raman lidar at observatory of Haute-Provence, Journal of Atmospheric and Oceanic Technology, 26(10), 2149-2160, 2009, DOI: 10.1175/2009JTECHA1287.1

Sherlock V., A. Garnier, A. Hauchecorne, and P. Keckhut, Implementation and validation of a Raman lidar measurement of middle and upper tropospheric water vapor, *Applied Optics*, 38, 5838-5850, 1999.

Hoareau, C., P. Keckhut, J.-L. Baray, L. Robert, Y. Courcoux, J. Porteneuve, H. Vömel, and B. Morel, A Raman lidar at la Reunion (20.8° S, 55.5° E) for monitoring water vapor and cirrus distributions in the subtropical upper troposphere: preliminary analyses and description of a future system, Atmos. Meas. Tech., 5(6), 1333-1348, 2012, doi:10.5194/amt-5-1333-2012.

Vérèmes H., Payen G., Keckhut P., Duflot V., Baray J.-L., Cammas J.-P., Evan S., Posny F., Körner S., Bosser P., Validation of the water vapor profiles of the Raman lidar at the Maïdo observatory (Reunion Island) calibrated with global navigation satellite system integrated water vapor, *Atmosphere*, MDPI 2019, 10, pp.713. ⟨10.3390/atmos10110713⟩.

3. A common Lidar retrieval algorithm implemented

3.1. Introduction

The water vapor profile was defined as one target component of the NDACC (Network for Detection of Atmospheric Composition Changes). The NDACC lidar group selected Raman method for water vapor and exchanges experiences between groups to achieve such a challenge.

The Raman lidar technique is a refinement of the lidar method that permits the profiling of the water vapor mixing ratio with high resolution and accuracy. These informations can be used to better understand the humidity conditions accompanying the contrails construction process and Persistence.

Using a standard high-power laser useful information can be extracted from some portion of the spectrum of the atmospheric backscattered signal.

Water vapor information can be derived from the Raman lidar backscatters in photon counting system (PCS) as described by Sherlock et al. (1999a), Hoareau et al. (2009), received at specific wavelengths corresponding to water vapor and nitrogen molecules during nightly seances in the absence of low clouds.

Lidar water vapor measurements have also some limitations, as it probes the atmosphere to get a humidity content that gets smaller with altitude until a very sensitive variability around the tropopause. Hence, a careful calibration is needed, using co-located external vertical profile measurements from Radiosondes, CFH sondes, models etc, or even total integrated humidity content as from GNSS.

One of the main challenges of the current treatment is the choice of improved Calibration method and to carefully consider the calibration uncertainty, to be adapted in order to unify the treatment protocole over multi lidar sites on the French territory, in spite of different acquisition modes and telescope FOV over these sites. Hereafter a brief description of the treatment method and the suggested calibration strategy is given.

This project has received funding from the European Union's Horizon Europe Research and innovation program under Grant Agreement No 101056885

3.2. Water Vapor Mixing Ratio « WVMR » Equation

Raman measurements are performed with the ratio of the Raman water vapor channel and the Nitrogen Raman Channel (Sherlock et al.,1999a). Then a direct measurement of the water vapor mixing ratio is obtained.

In order to get water vapor mixing ratio profile, Raman backscattered signals returned respectively at 607 (or 387) nm by Nitrogen and at 660 (or 408) nm by atmospheric water vapor are used, corrected for background noise, accounting for the atmospheric differential transmission T(z) and scaled by the calibration coefficient C (to be detailed later). Signals are measured by number of photons/bin/shot as following:

$$WVMR(z) = C \cdot T(z) \cdot \frac{S_{H_2O}(z) - B_{H_2O}(z)}{S_{N_2}(z) - B_{N_2}(z)}$$

Where :

C : The Calibration factor

$T(z)$: The atmospheric differential transmission

$S_{H_2O}(z)$: H_2O Raman signal

$B_{H_2O}(z)$: H_2O Raman Background signal noise

$S_{N_2}(z)$: N_2 Raman signal

$B_{N_2}(z)$: N_2 Raman Background signal noise

$S_{H_2O}(z) - B_{H_2O}(z)$: H_2O Cleaned signal

$S_{N_2}(z) - B_{N_2}(z)$: N_2 Cleaned signal

It has been shown that the relative transmission of the Raman returns due to the cirrus clouds is negligibly small for altitudes above 4 km. Consequently, no attenuation corrections have been applied (Sherlock et al. 1999a) .

3.3. Lidar Traitement Channel

3.3.1. Optical and periodic Integrations

The statistical nature of the incoherent laser soundings requires (for a given altitude) raw data being integrated over a number of laser successive shots and hence improve the signal to noise ratio SNR. More simply, each integration period consists of the photon counts of certain number of shots (8000 for OHP) for each altitude bin of few meters (75m for OHP, 15m for IPRAL, and so on), these counts constitute a signal profile with altitude.

Previous studies (Hoareau et al. 2009, Dionisi et al.2015) have determined the least total integration period as about 27 minutes of consecutive measurements, This should allow to consider the air masse stability and describe a vertical water vapor profile. The current treatment will be based on hourly screening to get a vertical profile that might reach an altitude of 12 km, longer periods might result in a several atmospheric situations mixed-up unrealistic profile. This hourly profile choice enable the calibration and avoid to lost interesting information about the variability of the local concentration. In some cases, another pre-filtering is applied to get only night measurements if the system operates with a day/night continuous rythme (like for IPRAL).

This project has received funding from the European Union's Horizon Europe Research and innovation program under Grant Agreement No 101056885

3.3.2. Noise correction

Atmospheric signals, particularly H_2O and N_2 ones exhibit inherent noise, that can obscure valuable information, accurate estimation of this noise is essential. Skylight background noise B_x is due to skylight brightness, thermal noise of the multiplier and signal-induced noise of a large initial burst.

The statistical distribution of photon pulses is expected to follow the « Poisson distribution », Note that Water vapor Raman signals are two order of magnitude smaller than Nitrogen Raman signals. However Noise magnitude is not likely to follow the same logic, see figure 1.

Historical Lidar SNR analysis for the period between 2001-2010 show that most signal above 20 km from H_2O wavelengths and above 50 km for N_2 wavelengths are assumed to primarily comprise noise.

Hence, The background noise model is estimated as the median of the photon counts (signal) for altitudes > 20 km for H_2O signal noise, and > 50 km for N_2 one.

The error associated with noise calculation is estimated using statistical bootstrapping, a specific number of bootstrapped iterations (default: 1000) are performed to generate resampled datasets, from which bootstrapped medians are computed, the standard deviation of the bootstrapped medians provides an estimate of the error in the noise calculation.

3.3.3. Signal Cleaning

Lidar raw signals have to be smoothed to enhance their quality. An adaptive Blackman window filtering is tailored to accommodate varying altitudes and signal characteristics. Filter window sizes are adjusted based on altitude while a decay factor is incorporated beyond specified altitude limits according to the signal magnitude. The vertical resolution remained unchanged.

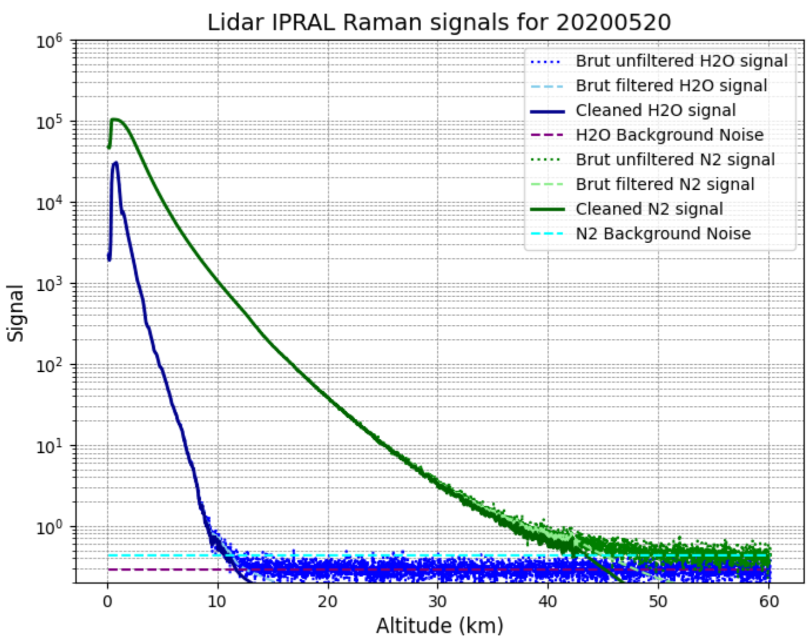

Figure 9. Example of Raman lidar signals: Brut, filtered, cleaned with the associated noises, Blues for H2O , and greens for N2 .

This project has received funding from the European Union's Horizon Europe Research and innovation program under Grant Agreement No 101056885

Cleaned signal is the lidar signal resulting after signal smoothing and noise removing process, the signal cleaning is assuring that only relevant signal components are retained. Subsequently, the cleaned signal undergoes interpolation to handle zero or negative values (altitudes of SNR <=1). Such outlier values are replaced with interpolated values from neighboring positive data points and decaying towards zeros.

See figure 9 for an example of the raw and cleaned Raman signals of a full night integrated measurements and their noise level. Water vapor signal is shown to extend up to 11 km for this exemple. While nitrogen signal is detectable up to about 43 km.

3.4. WVMR Error estimation

Most of the lidar methods are based on a ratio of two simultaneous signals, and thus immune to long term instrumental drift and measurement conditions. Systematic errors are expected to be reduced by hard-ware design, Thus, the signal processing related to measurement uncertainties is based on random errors (Sherlock et al.1999). The two principal error sources considered here are photon counting and skylight background estimation, one evident extra error source will be related to the calibration factor estimation.

3.4.1. Signal Detection Error

The Signal detection error (also referred to as photon-counting error) process is described by Poisson statistics, and the standard deviation of the measurement is $\sigma = \sqrt{N}$, where N is the number of photons counted. This error represents the uncertainty in determining the WVMR due to inherent variations and noise in the lidar signals. It is estimated based on the cleaned signals of H_2O and N_2, along with the brut signals respective detection errors. The detection error is calculated as the root mean square (RMS) of the relative errors associated with H_2O and N_2 signals, adjusted by their respective noise levels. This provides a comprehensive assessment of the detection error in the WVMR estimation process as following:

$$WVMR_{\text{detection\_err}} = \sqrt{\left(\frac{1}{\left(S_{N_2}(z) - B_{N_2}(z)\right)} \cdot S_{H_2O,err}(z)\right)^2 + \left(\frac{S_{H_2O}(z) - B_{H_2O}(z)}{\left(S_{N_2}(z) - B_{N_2}(z)\right)^2} \cdot S_{N_2,err}(z)\right)^2}$$

Where :

$S_{N_2}(z)$: N_2 Raman signal

$B_{N_2}(z)$: N_2 Raman Background signal noise

$S_{N_2}(z) - B_{N_2}(z)$: N_2 Cleaned signal

$S_{H_2O,err}(z)$: H_2O Raman brut signal detection error

$S_{N_2,err}(z)$: N_2 Raman brut signal detection error

$S_{H_2O}(z) - B_{H_2O}(z)$: H_2O Cleaned signal

This project has received funding from the European Union's Horizon Europe Research and innovation program under Grant Agreement No 101056885

3.4.2. Noise Detection Error

Similar to the detection error, the noise estimation error is calculated using RMS of the relative errors, reflecting the combined impact of noise estimation inaccuracies on WVMR calculations. The noise estimation error is computed using the following equation:

$$WVMR_{\text{noise\_err}} = \sqrt{\left(\frac{1}{\left(S_{N_2}(z) - B_{N_2}(z)\right)} \cdot B_{H_2O,err}(z)\right)^2 + \left(\frac{S_{H_2O}(z) - B_{H_2O}(z)}{\left(S_{N_2}(z) - B_{N_2}(z)\right)^2} \cdot B_{N_2,err}(z)\right)^2}$$

Where :

$S_{N_2}(z)$: N_2 Raman signal

$B_{N_2}(z)$: N_2 Raman Background signal noise

$S_{N_2}(z) - B_{N_2}(z)$: N_2 Cleaned signal

$B_{H_2O,err}(z)$: H_2O Background noise estimation error

$B_{N_2,err}(z)$: N_2 Background noise estimation error

$S_{H_2O}(z) - B_{H_2O}(z)$: H_2O Cleaned signal

3.4.3. Calibration Error

This error is the RMSE between the Calibrated Lidar profile and the referenced profile for calibration, taking into account both profile portions between 3 and 5 km of altitude (calibration zone).

3.4.4. WVMR total Error

The total WVMR error is calculated for certain period (hour or even full night), taking into account 3 sources of uncertainty and variability in the measurements:

I. **Calibrated Detection Error**: The detection error (section 4.2), representing the uncertainty in detecting and quantifying the WVMR signal, is calibrated to reflect the scaling factors for this hour (or night).

Calibrated Detection Error = $WVMR_{\text{detection\_err}} / Calibration_{\text{factor}}$

II. **Calibrated Noise Error**: The noise estimation error (section 4.3) is first calibrated to account for any scaling factors. This calibration process adjusts the noise error for the hour (or night) based on the corresponding calibration factor.

Calibrated Noise Error = $WVMR_{\text{noise\_err}} / Calibration_{\text{factor}}$

III. **Calibration Error**: The error introduced during the calibration process itself is considered. This error accounts for any discrepancies or inaccuracies in the calibration procedure, impacting the final WVMR estimation.

Calibration error = $WVMR_{\text{Calibration\_err}} * WVMR$

This project has received funding from the European Union's Horizon Europe Research and innovation program under Grant Agreement No 101056885

The total WVMR error is the sum of the previous three errors, see figure 2.

$$WVMR_{\text{Total\_err}} = WVMR_{\text{detection\_err}}/Calibration_{\text{factor}} + WVMR_{\text{noise\_err}}/Calibration_{\text{factor}} + WVMR_{\text{Calibration\_err}}*WVMR$$

3.5. Lidar Calibration

Water vapor mixing ratio as a physical parameter is proportional to the ratio of the H_2O and N_2 raman channels signals. The calibration process is conducted to give a geophysical meaning of this ratio to be converted on a real WVMR profile by a scale factor. The application of lidar measurements to climatological study requires a robust calibration of the instrument. Different calibration methodologies have been developed (Whiteman et al., 2006; Leblanc et al., 2012; Hoareau et al., 2009; Dionisi et al., 2010; Bock et al., 2013). Two principal ways are known to calculate this conversion factor (calibration factor):

- Internal method: this method consists of calculating/measuring each term composing the calibration constant, each representing a source of incertitude in relevant parameters of the lidar system (ex: temperature dependance of the Raman cross-section) to be measured or calculated experimentally using standard laboratory procedures (Sherlock et al.,1999, Venable et al.,2011). This method presents larger margins of errors accumulated, and is thus less recommended when accurate measurements are requested.
- External method: this method estimates the total calibration coefficient as the ratio between a reference instrument, and the uncalibrated lidar data and the calibration therefore depends on the accuracy of another instrument that also presents its own limitations.
    - o Co-axial systems: Calibration using a referenced TCWV quantities, as for OPAR (La réunion island - France (Hoareau et al.,2012; Dionisi et al.,2015; Vérèmes et al.,2019). GNSS integrated water vapor quantity is used to get the calibration factor (the coincident integrated water vapor lidar quantity is calculated and the ratio of both quantities for certain period is considered as the scale factor of the period).
    - o Bi-axial systems : Calibration using referenced WVMR profil, as for OHP and IPRAL lidars. Since the lidar profile is not extended to sol, the reference need to provide a vertical WVMR profile, to enable a comparaison for certain zone of the profile and hence calibrate the full profile. This method can also be applied to calibrate co-axial lidars, so it is chosen to unify the calibration strategy over the four lidars on the French territories.

3.5.1. Reference choice

Many techniques are capable to provide WVMR referenced profiles for lidar calibration, like Radiosondes, laser Diodes, CFH, balloon-borne frost-point Hygrometers, or FTIR measurements on meteorological stations (Bock et al., 2013, Dionisi et al.,2015, Leblanc et al.,2012, Vowel et al.,2007, Meyer et al.,2015). These instruments have their potential as references to describe WVMR in the troposphere but they have also their limitations. Starting from expensive long-term operational costs, and passing by limited accuracy on upper troposphere, it's very complicated to find the suitable instrument for a long term calibration strategy.

The French sites are supplied with radiosondes measurements twice a day (midnight and midday lunchs) which provide a well qualified data set but found to have a serious limitation of discontinuities at individual stations (humidity sensor response, material change, etc.) and a poor sensitivity in the upper troposphere due to the radiosonde derivation from the zenith above the site by wind. Also, radiosondes don't give a sufficient temporal coverage to calibrate a short time WVMR

This project has received funding from the European Union's Horizon Europe
Research and innovation program under Grant Agreement No 101056885

profile (hourly fro exemple) and detect thereby an interesting events on the above site air-masse, hence hourly calibration references profiles are needed.

The ECMWF latest hourly re-analyses datasets named ERA-5 (Hersbach et al.,2023), represents the fifth generation of the European Centre for Medium-Range Weather Forecasts – ECMWF reanalysis, providing a comprehensive overview of global climate and weather spanning the past eight decades. Data is accessible from 1940 onwards, marking a transition from the previous ERA-Interim reanalysis. Gridded data provided by ERA5 have a horizontal resolution of 0.25° x 0.25°. It provides vertical coverage between 1000 hPa to 1 hPa, with a vertical resolution of 37 pressure levels, and hourly temporal resolution (Hersbach et al., 2023).

Forced by radiosondes, ERA-5 shows a good quality to make climatological studies, but are suspected to miss local short term events too. Trying to assess the limitations of these re-analyses with respect to the radiosondes, the results show a dry radiosonde bias that gets more important with altitude, the best agreement being found on altitudes between 3 and 5 km see Figure 10.

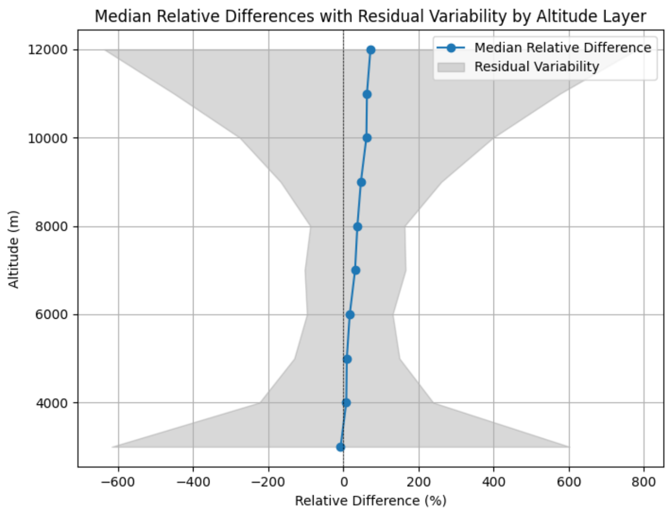

Figure 10. Relative Error (ERA-5 ,MF-Radiosonde) of Relative humidity profiles cases coincident to lidar measurements (OHP: 2001-2010) and the residual variability.

3.5.2. Calibration Method

Collocated and simultaneous Lidar water vapor mixing ratio (WVMR) hourly profiles (Level 2) from cleaned signals (Level 1) are calibrated using hourly ERA-5 reanalysis data, between 3 & 5 km. The collocated 37 pressure levels reference is considered allowing a maximal spatial drift of 0.1° and the best temporal coincident (same lidar measurements dominant hour). The Extern calibration strategy undergoes the following steps:

Altitude Range Selection: The calibration process focuses on a specific altitude range, typically between 3 to 5 kilometers above ground level (km). This range is chosen to ensure that calibration factors are derived from regions of the atmosphere where both lidar and ERA5 hourly data exhibit reliable measurements.

Data Preparation: The ERA-5 profiles are prepared by reversing their altitude arrays to match the ascending altitude sequence of the lidar instrument. The ERA5 profile within the calibration range is interpolated onto the lidar altitude grid. Altitude and profile data within the selected calibration range are extracted from both datasets for further processing.

Calibration Factors Calculation: Calibration factors are then calculated by dividing the lidar WVMR profiles by the interpolated ERA5 profiles. These calibration factors represent the scaling factors

This project has received funding from the European Union's Horizon Europe Research and innovation program under Grant Agreement No 101056885

required to align the lidar measurements with the ERA5 reference data within the selected altitude range.

Hourly Profile Calibration: The entire lidar altitude profile calibration is obtained as the mean of the calibration factors of the selected altitude range. This process ensures that the entire lidar profile is calibrated consistently with one hourly calibration factor.

Error and uncertainties Estimation: The calibration process includes the estimation of calibration errors to quantify the discrepancies between the calibrated lidar profiles and the ERA5 reference data. Root Mean Squared Error (RMSE) and correlation coefficient metrics are calculated to assess the accuracy and reliability of the calibration process.

Full night Calibration & validation: Hourly Calibration factors which are issues of significantly correlated hourly WVMR lidar profiles lidar to ERA-5 ones between 3 & 5 km, are averaged each night of measurement and are named nightly coefficient. Nightly calibrated profiles are validated against colocated radiosondes ones when possible, I.e corrected radiosondes dataset (Dupont et al.,2020).

Full period Calibration & validation: The evolution of the calibration coefficient over a long enough period permits one to adjust the series to instrumental changes that are unavoidable in a long commitment (ageing and/or substitution of filters, fiber- optic, receiving optic alignment, detectors, etc.). The average nightly coefficient between two instrumental changes detected is considered as the “calibration coefficient” of each measurement performed during this period.

Figure 11 describes the treatment channel from the shortest integrated Raman signals (Level 0 or Brut data) to the calibrated full period WVMR profiles (Level 3: full nights profiles calibrated with the same calibration factor as belongs to a stationary period: archived data), passing by the hourly summed cleaned data (level 1) and quasi-real time uncalibrated hourly WVMR (level 2a), and the hourly calibrated ones(Level2b). While Figure 12a illustrates two exemples of WVMR profiles obtained from lidar measurements at OHP (left) and at SIRTA (right), where radiosondes (Meteo-France M10) WVMR profiles (black) show a clear wet bias compared to colocated ERA-5 re-analysis profile (magenta) used for calibration of Lidar uncalibrated profile (red), and thereby with respect to the calibrated lidar profile (green) presented also along with the associated errors (green shadows).

The upper panel of figure 12a depicts one-hour (midnight) Water Vapor Mixing Ratio (WVMR) profiles acquired from lidar measurements, along with the calibration references ERA-5 and the nearest collocated Meteo-France (M10) Radiosonde profile for the midnight hour for validation purposes. The panel is zoomed to provide a detailed view of the lower profile portion between 3 and 5 km altitude, which serves as the calibration range. Lidar profiles are significantly correlated (80%) to radiosondes on the calibration range (3-5 km), and best to ERA-5(around 99%)..

The middle panel extends the analysis to show WVMR profiles up to 10 km altitude for the same hour. Uncalibrated & calibrated lidar, ERA-5, and Radiosonde profiles are presented, offering a comprehensive view of the atmospheric water vapor distribution over an extended altitude range. Hourly calibrated lidar profiles (up to 12 km) are significantly correlated to the collocated radiosonde ones by 65% and 70% at SIRTA (IPRAL) and OHP respectively. A much better correlation to ERA-5 is noted (better than 90% on both sites).

The bottom panel provides a holistic view of the full-night calibrated WVMR profiles, capturing the variations in water vapor content throughout the night (3, 6 hours integrated at IPRAl, OHP respectively). The inclusion of collocated radiosonde data (midnight) facilitates validation of the calibrated lidar measurements. The added ERA-5 profile is that of the mid-night hour (to be coinciding with radiosonde one).

Figure 12b illustrates two other examples of WVMR profiles obtained from other dates lidar measurements at OHP (left) and at SIRTA (right), where radiosondes (Meteo-France M10) WVMR profiles (black) show this time a clear dry bias (as expected from previous studies and most case studies, So that smaller RS magnitudes are observed compared to collocated ERA-5 re-analysis profile

This project has received funding from the European Union’s Horizon Europe
Research and innovation program under Grant Agreement No 101056885

(magenta) used for calibration of Lidar uncalibrated profile (red), and thereby with respect to the calibrated lidar profile (green) presented also along with the associated errors (green shadows).

The three panels have similar signification as those of figure 12a, with zoomed hourly WVMR profiles obtained between 3 and 5 km height for all three instruments in the upper panel, and an extended view of the WVMR profiles up to 10 km on the middle panel, and the full night lidar WVMR (6 hours integrated at each of IPRAl, OHP, total period centered at mid-night) presented with the mid-night colocated radiosonde and the coincident (to Radiosonde) ERA-5 hourly profile.

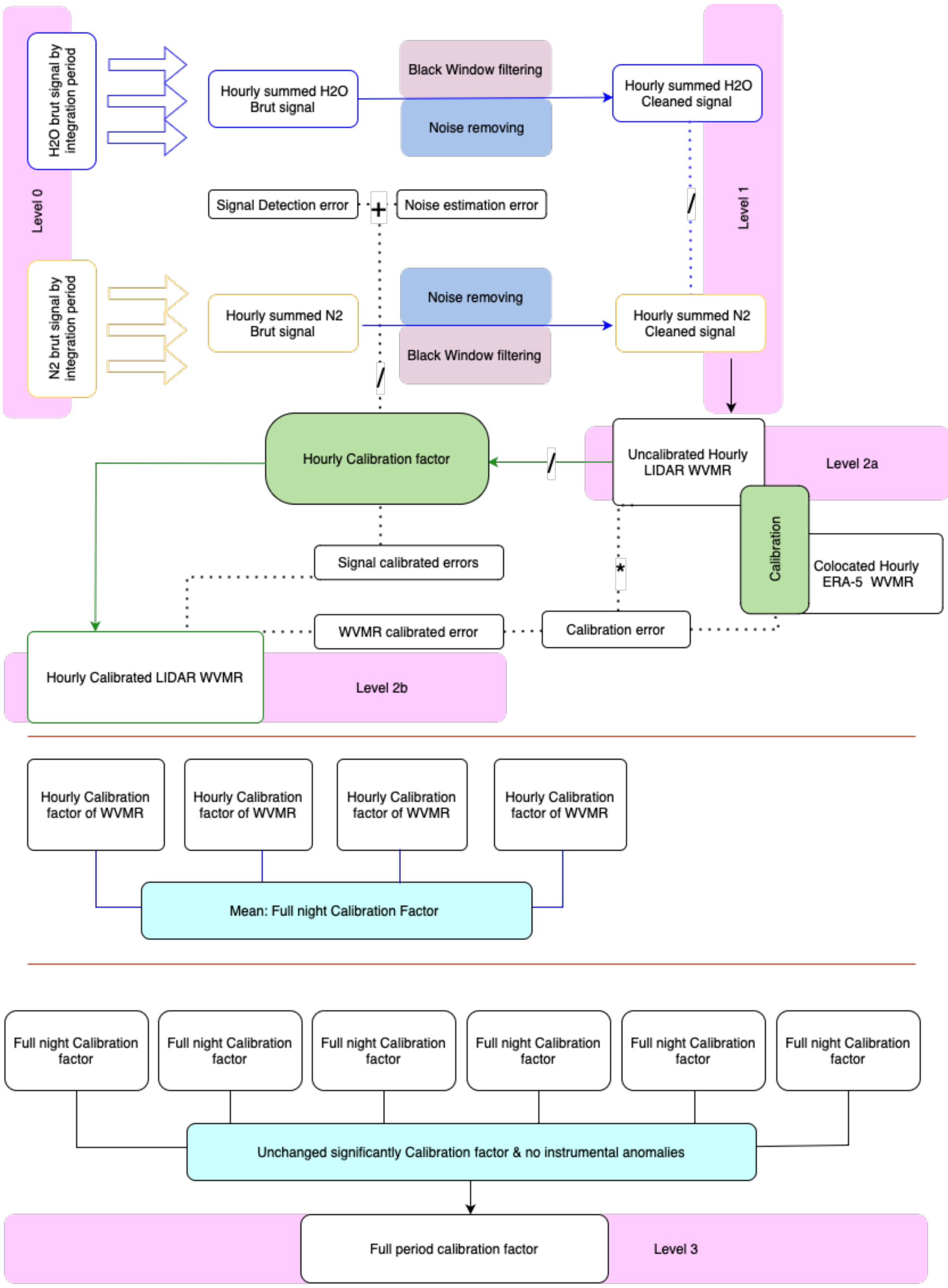

Figure11. Diagram of Raman Lidar Treatment channel using Externe Calibration Strategy via ERA-5 Hourly profiles.

This project has received funding from the European Union's Horizon Europe Research and innovation program under Grant Agreement No 101056885

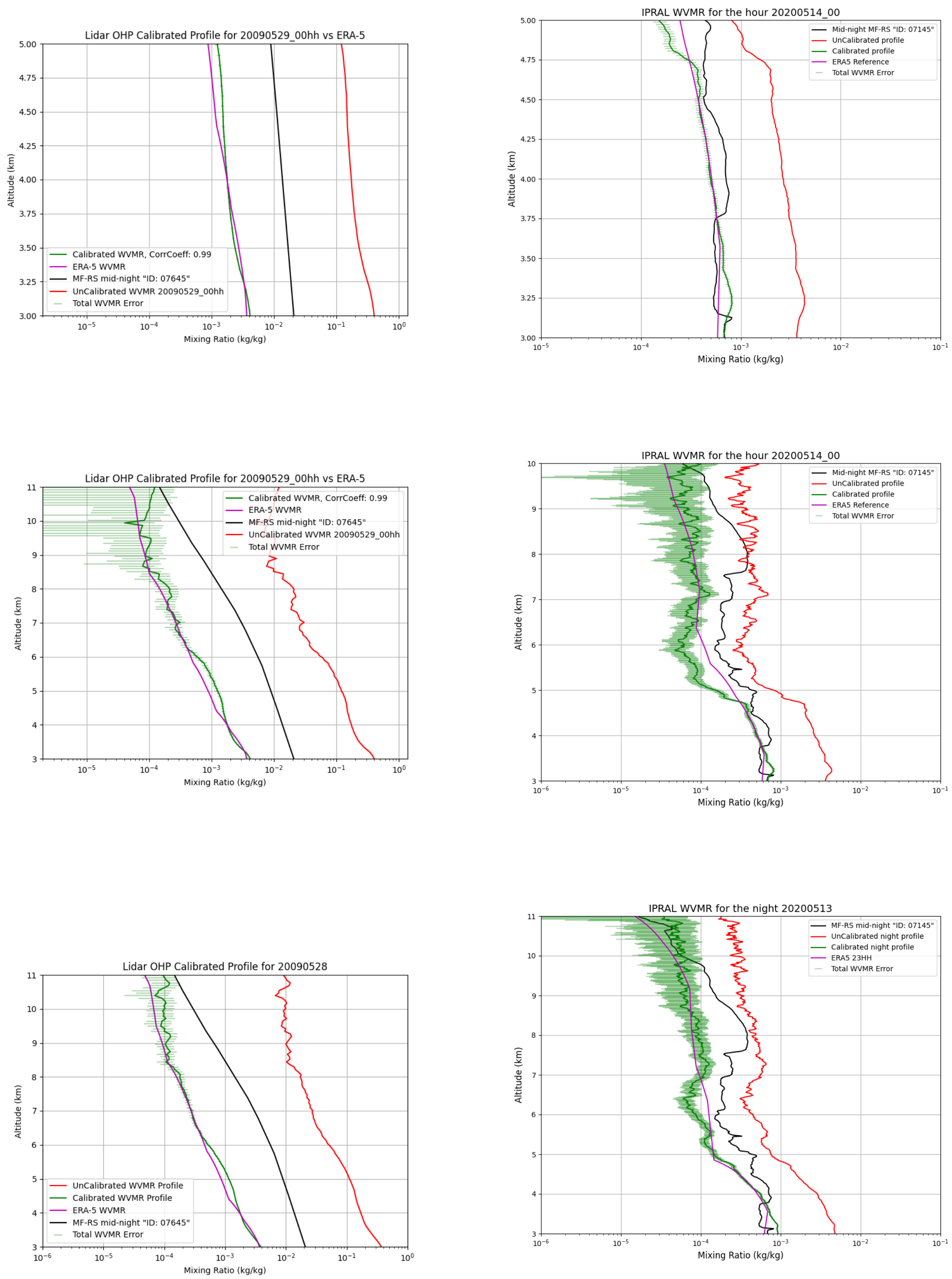

Figure12a. Exemple of Drier Raman Lidar full night WVMR profiles (than RS). Left for OHP, Right for IPRAL lidar calibrated using Externe Calibration Strategy via ERA-5 Hourly profiles. Upper figure: midnight hourly calibration profiles between 3 & 5 km, middle figure: same hour extended profile up to 10 km, bottom: full night calibrated profile. Legends: In red is the uncalibrated lidar profile, in green the calibrated one, in black the colocated Meteo-France (M10) radiosonde mid-night WVMR profile, in magenta the hourly ERA-5 colocated calibration reference, total WVMR errors are represented in green shadows.

This project has received funding from the European Union's Horizon Europe Research and innovation program under Grant Agreement No 101056885

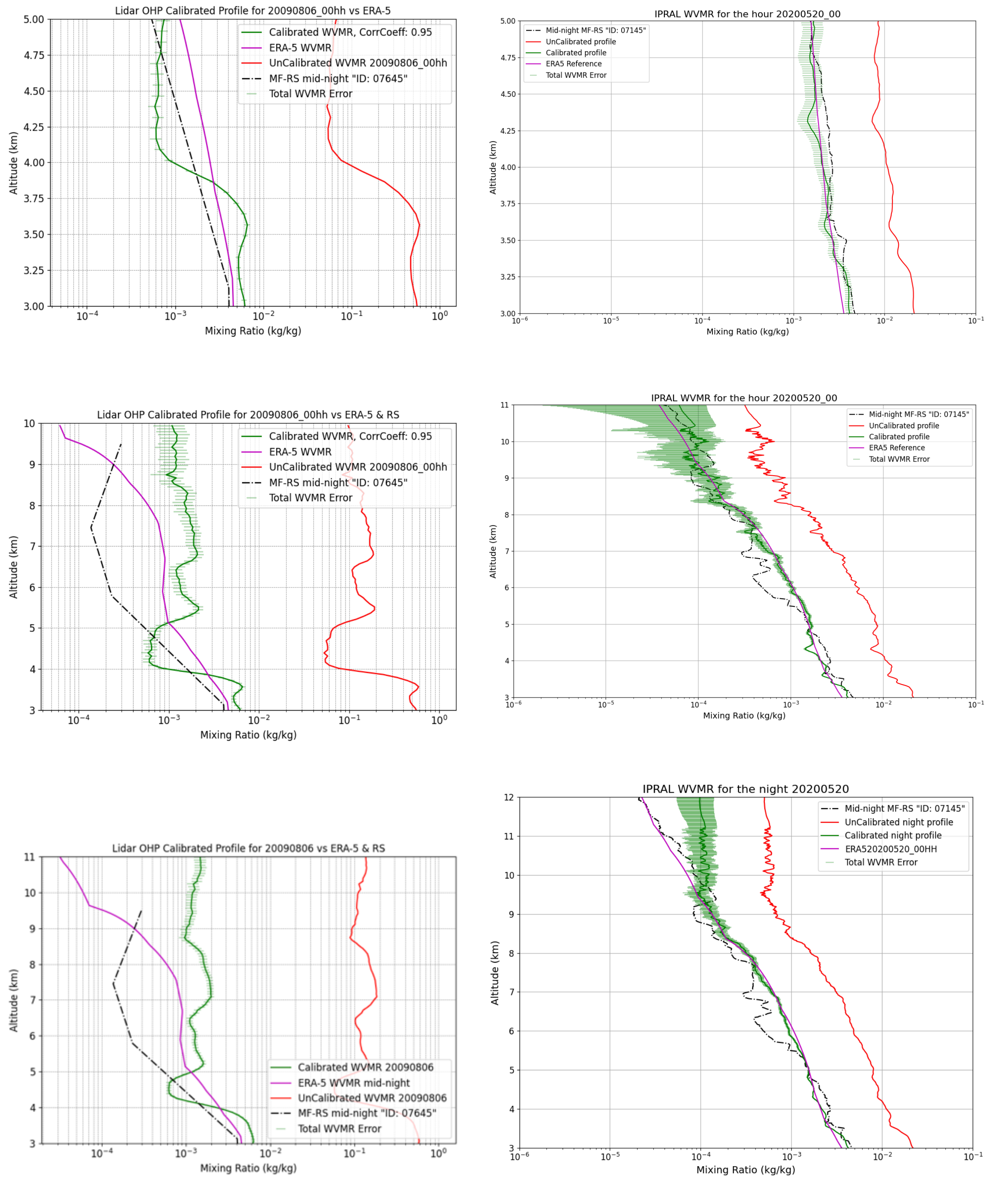

Figure12b. Exemple of more humide Raman Lidar full night WVMR profiles (compared to RS) . Left for OHP, Right for IPRAL lidar calibrated using Externe Calibration Strategy via ERA-5 Hourly profiles. Upper figure: midnight hourly calibration profiles between 3 & 5 km, middle figure: same hour extended profile up to 10 km, bottom: full night calibrated profile. Legends: In red is the uncalibrated lidar profile, in green the calibrated one, in black the collocated Meteo-France (M10) radiosonde mid-night WVMR profile, in magenta the hourly ERA-5 collocated calibration reference, total WVMR errors are represented in green shadows.

This project has received funding from the European Union's Horizon Europe Research and innovation program under Grant Agreement No 101056885

The overall agreement between radiosonde, ERA-5 and full night lidar profiles (figure 12b), as well as the vertical variability in water vapor content within the atmosphere by the different techniques is figured out. Lidar and Radiosondes profiles up to 12 km are significantly correlated at 70% (OHP) and at 74% (SIRTA). Lidar and ERA-5 profiles are significantly correlated (more than 95% on both sites).

3.6. Conclusions

This deliverable describes the universal calibration approach to be adopted, leveraging co-located ERA-5 hourly water vapor profiles assimilating radiosonde data from the lower troposphere. Hourly integration periods of lidar water vapor mixing ratio (WVMR) are compared with corresponding ERA-5 re-analyses, with hourly calibration factors from which nightly calibration factors are derived. Daily calibrations are scrutinized to identify any instrumental effects on calibration coefficients, with final coefficients calculated for quasi-stationary periods. Additionally, at certain sites, collocated radiosondes observations are examined and compared with ours.

In conclusion, the methodology presented herein exhibits versatility, applicable across diverse sites, although its ultimate refinement requires a comprehensive dataset for calibration. Encouragingly, our results exhibit a robust agreement with both ERA5 reanalysis and Metro France Modem 10 radiosonde observations within the lower troposphere (3-7 km), thereby validating its efficacy in this altitude regime. However, preliminary analyses suggest a potential underestimation of water vapor by ERA5 at higher altitudes (>10 km), necessitating deeper uncertainty assessment, is conducted in section 4. Further investigation and refinement in subsequent project phases.

The newly developed software enables valuable insights into humidity content within the 7-11 km range, crucial altitudes for potential contrail formation. This software will advance our comprehension of contrail formation and persistence dynamics, and the potential impact of contrails on future air traffic regulation.

3.7. References

Bock, O., Bosser, P., Bourcy, T., David, L., Goutail, F., Hoareau, C., Keckhut, P., Legain, D., Pazmino, A., Pelon, J., Pipis, K., Poujol, G., Sarkissian, A., Thom, C., Tournois, G., and Tzanos, D.: Accuracy assessment of water vapour measurements from in situ and remote sensing techniques during the DEMEVAP 2011 campaign at OHP, Atmos. Meas. Tech., 6, 2777–2802, 2013..〈10.5194/amt-6-2777-2013〉

Dionisi, D., F. Congeduti, G. L. Liberti, and F. Cardillo, 2010: Calibration of a Multichannel Water Vapor Raman Lidar through Noncollocated Operational Soundings: Optimization and Characterization of Accuracy and Variability. J. Atmos. Oceanic Technol., 27, 108–121,2010 〈10.1175/2009JTECHA1327.1〉

Dionisi, D., Keckhut, P., Courcoux, Y., Hauchecorne, A., Porteneuve, J., Baray, J. L., Leclair de Bellevue, J., Vérèmes, H., Gabarrot, F., Payen, G., Decoupes, R., and Cammas, J. P., Water vapor observations up to the lower stratosphere through the Raman lidar during the Maïdo lidar calibration campaign, Atmos. Meas. Tech., 8, 1425-1445.〈10.5194/amt-8-1425-2015〉

Dupont, J., M. Haeffelin, J. Badosa, G. Clain, C. Raux, and D. Vignelles, 2020: Characterization and Corrections of Relative Humidity Measurement from Meteomodem M10 Radiosondes at Midlatitude Stations. *J. Atmos. Oceanic Technol.*, **37**, 857–871, 〈10.1175/JTECH-D-18-0205.1〉.

This project has received funding from the European Union's Horizon Europe
Research and innovation program under Grant Agreement No 101056885

Hersbach, H., Bell, B., Berrisford, P., Biavati, G., Horányi, A., Muñoz Sabater, J., Nicolas, J., Peubey, C., Radu, R., Rozum, I., Schepers, D., Simmons, A., Soci, C., Dee, D., Thépaut, J-N. (2023): ERA5 hourly data on pressure levels from 1940 to present. Copernicus Climate Change Service (C3S) Climate Data Store (CDS), (Accessed on DD-MMM-YYYY). 〈 10.24381/cds.bd0915c6〉

Hoareau, C., P. Keckhut, A. Sarkissian, J-L. Baray, And G. Durry, Methodology for water monitoring in upper troposphere with Raman lidar at observatory of Haute-Provence, Journal of Atmospheric and Oceanic Technology, 26(10), 2149-2160, 2009. 〈10.1175/2009JTECHA1287.1〉

Hoareau, C., P. Keckhut, J.-L. Baray, L. Robert, Y. Courcoux, J. Porteneuve, H. Vömel, and B. Morel, A Raman lidar at la Reunion (20.8° S, 55.5° E) for monitoring water vapor and cirrus distributions in the subtropical upper troposphere: preliminary analyses and description of a future system, Atmos. Meas. Tech., 5(6), 1333-1348, 2012. 〈10.5194/amt-5-1333-2012〉.

Leblanc, T., McDermid, I. S., and Walsh, T. D.: Ground-based water vapor raman lidar measurements up to the upper troposphere and lower stratosphere for long-term monitoring, Atmos. Meas. Tech., 5, 17–36, 2012.〈10.5194/amt-5-17-2012〉

Meyer, J., Rolf, C., Schiller, C., Rohs, S., Spelten, N., Afchine, A., Zöger, M., Sitnikov, N., Thornberry, T. D., Rollins, A. W., Bozóki, Z., Tátrai, D., Ebert, V., Kühnreich, B., Mackrodt, P., Möhler, O., Saathoff, H., Rosenlof, K. H., and Krämer, M.: Two decades of water vapor measurements with the FISH fluorescence hygrometer: a review, Atmos. Chem. Phys., 15, 8521–8538, 2015. 〈10.5194/acp-15-8521-2015〉

Sherlock V., A. Garnier, A. Hauchecorne, and P. Keckhut, Implementation and validation of a Raman lidar measurement of middle and upper tropospheric water vapor, *Applied Optics*, 38, 5838-5850, 1999.〈10.1364/AO.38.005816〉

Venable, D.D.; Whiteman, D.N.; Calhoun, M.N.; Dirisu, A.O.; Connell, R.M.; Landulfo, E. Lamp mapping technique for independent determination of the water vapor mixing ratio calibration factor for a Raman lidar system. *Appl. Opt.* **2011**, *50*, 4622–4632.〈10.1364/AO.50.004622〉

Vérèmes H., Payen G., Keckhut P., Duflot V., Baray J.-L., Cammas J.-P., Evan S., Posny F., Körner S., Bosser P., Validation of the water vapor profiles of the Raman lidar at the Maïdo observatory (Reunion Island) calibrated with global navigation satellite system integrated water vapor, *Atmosphere*, MDPI 2019, 10, pp.713. 〈10.3390/atmos10110713〉.

Vömel, H.; David, D.E.; Smith, K. Accuracy of tropospheric and stratospheric water vapor measurements by the cryogenic frost point hygrometer: Instrumental details and observations. *J. Geophys. Res. Atmos.* 2007, *112*. 〈10.1029/2007JD008698〉.

Whiteman, D. N., and Coauthors, 2006: Raman water vapor lidar measurements during the International H2O Project. Part I: Instrumentation and analysis techniques. *J. Atmos. Oceanic Technol*, **23 ,** 157–169.〈10.1175/JTECH1838.1〉

This project has received funding from the European Union's Horizon Europe Research and innovation program under Grant Agreement No 101056885

4. Evaluation of meteorological radiosondes over lidar experimental sites

4.1. Operational context

The study of the climatic impact of contrails is based on a good knowledge of the distributions of water vapor in the upper troposphere in order to determine as precisely as possible the zones of supersaturation.

Radiosondes are instruments that are used to measure various atmospheric parameters at different altitudes until the stratosphere, but measurements of very low water vapor content encountered above 10 km remain challenging (Dirksen et al., 2014, 2020).

It is therefore fundamental to properly quantify the sources of error and to optimize data processing to have the best possible water vapor measurements, which is one of the objectives of the Global Climate Observing System (GCOS) Reference Upper-Air Network (GRUAN), an international reference observing network of sites measuring essential climate variables above Earth's surface.

The meteorological radiosondes performed by Météo-France since 2011 are equipped with Modem M10 probes, which are also used in more than 28 countries (Dupont et al., 2020). Recently, since 2023, many Météo-france sites (including Nîmes-Courbessac, Trappers, Bordeaux-Mérignac, Brest-Guipavas, Ajaccio, Dumont D'Urville, Kerguelen, Cayenne-Matoury, Hiva-Oa, Faaa, Rapa, Noumea, Gillot, Le Raizet and Mangareva). have switched to the M20 Modem probe. The evolution from M10 to M20 should allow the quality of measurements to be improved and the uncertainty to be reduced.

On the basis of intercomparisons with other sonde types (including Vaisala RS92 and RS41), studies performed within the framework of GRUAN proposed reprocessing methods of the M10 radiosondes in order to reduce the bias and uncertainty of these measurements, which are due to.

- Calibration of the probe

- The time-response of the sensor when subjected to sudden changes of humidity

- The dependence of RH sensors on temperature

Dupont et al. (2020) showed that uncertainties in relative humidity can be reduced by 4% by applying probe reprocessing.

Information on atmospheric humidity on a global scale is also available in the ERA-5 reanalysis of the European center ECMWF which can be extracted at 0.125° horizontal resolution, at a hourly temporal resolution and on 137 vertical model levels.

In the following section (4.2) we will present statistical comparisons between Modem M10 radiosonde and humidity profiles extracted from the ERA-5 ECMWF reanalysis.

4.2. Comparisons between radiosondes and ERA5 model

4.2.1. Methodology

In order to determine and quantify possible measurement biases between the M10 probes and ERA5, we calculated the monthly average profiles on several Meteo-France sites located in France (Trappes, Bordeaux, Nimes). We present here the Nimes station (43.87°N, 4.40°E) which is close to the Haute Provence observatory (ACTRIS and NDACC site).

This project has received funding from the European Union's Horizon Europe Research and innovation program under Grant Agreement No 101056885

The M10 profiles are directly compared to ERA5 profiles interpolated at the location of the radiosonde launch point. Indeed, the initial investigations focused on ERA5 data interpolated along one dimension, meaning that we used data from the grid point closest to the Nîmes station. After examining the isobaric fields of relative humidity around the Nîmes station, we noticed that relative humidity often varied significantly spatially. Consequently, we linearly interpolated the ERA5 data based on the latitudinal and longitudinal movements of the radiosonde balloons.

We considered only the M10 data obtained during the ascent of the balloon before its explosion, (on average at 25 km). two radiosonde launches are performed every day, one during the night (11:15 p.m.) and the other during the day (11:15 a.m.). The maximum duration of the radiosondes is 1 hour 45 minutes, and the vertical resolution is 10 m on average, corresponding to around 2000 points. The ERA5 reanalysis data have been extracted at 0.25° horizontal resolution and 1h temporal resolution.

4.2.2. Results

Figure 13 shows monthly mean values of relative humidity over Nimes obtained by Modem M10 probes and ECMWF ERA5 outputs in January and July 2022, separating day and night data. The results show a good agreement in the lower troposphere, less than 5% of difference between the ground level and approximately 500 hPa (400 hPa in July at night). Near the tropopause region, the difference between sondes and ERA5 increase, reaching 12 to 25% between 200 and 400 hPa pressure levels This humidity difference is larger during the day than during the night (22%/11%) and in winter than in summer (21%/15%).

When comparing the 2021 data (ERA5 and M10), we observed a similar bias to that of 2022 in the Upper Troposphere and Lower Stratosphere (UTLS) for both datasets. Specifically, in the lower troposphere (500-900 hPa), we observed good agreement between ERA5 and radiosonde data in 2021, like what was observed in 2022, across four different periods (January - day/night, July - day/night). However, in the UTLS region, we identified a deviation of over 8% in January (night, 2022) compared to January (night, 2021) between ERA5 and radiosonde data. For all other periods (January - day, July - night/day), no significant difference was observed between the biases identified in 2022 and 2021 in the UTLS.

We evaluated data from two additional radiosonde stations (Bordeaux and Trappes) to determine if the discrepancy could vary from one station to another. In the lower troposphere, a good agreement was observed between ERA55 and radiosonde data from both stations (Bordeaux, Trappes). However, in the UTLS, variations were noted, with a bias of 2% compared to Nîmes for both stations in January (night), 10% in January (day), and 10% in July (day) in Bordeaux. For the Trappes station compared to Nîmes, differences of +10% in July (night) and +5% for January and July (day) were observed. Despite these differences between radiosonde stations, these studies do not explain the identified humid bias in the UTLS.

Virman et al., (2021) made a comparative study of radiosonde M10 with ERA5 above 8 stations located in the west of the Pacific Ocean and in the east of the Indian Ocean over the period from November to February between 1998 and 2014. They showed that on most stations, ECMWF ERA5 had a wet bias of 2-6% on radiosonde between 650 and 800 hpa. Between 300 and 500 hPa the wet bias of ERA-5 reached 14% in some stations.

This project has received funding from the European Union's Horizon Europe Research and innovation program under Grant Agreement No 101056885

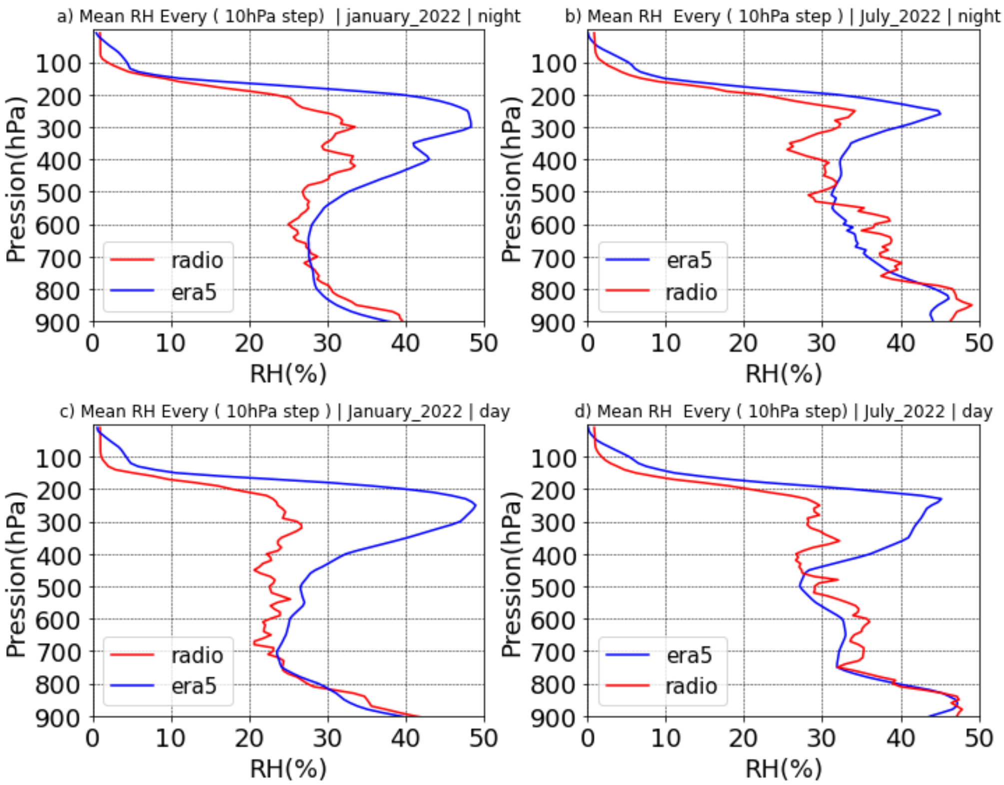

Figure 13 : Vertical mean profiles of M10 radiosonde (in red) and ECMWF ERA-5 (in blue) relative humidity at Nimes during the night in January 2022 (a) and July 2022 (b), and during the day in January 2022 (c) and July 2022 (d).

Figure 14 focuses on the distributions of relative humidity values in the zone of potential cirrus/contrail formation between 200-300 hPa. ECMWF (ERA5) clearly presents more wet situations than radiosondes which shows almost no sur-saturation value (more than 100%). At this stage, we cannot know to what extent ECMWF (ERA5) overestimates humidity, or the radiosonde underestimates it.

In section 4.1 we mention that GRUAN had proposed a reprocessing of the radiosonde to improve their quality. Figure 15 shows the comparison between the average vertical profiles of the radiosonde with and without the GRUAN correction and ECMWF ERA5 reprocessing.

In the lower troposphere, at night, up to 500 hPa, the GRUAN correction reduces significantly the difference with ERA5 (2-5% difference between ERA5 and GRUAN compared to 2-12% between ERA5 and METEO-FRANCE). During the day and in this altitude range, the GRUAN correction has little influence. In the upper troposphere and lower stratosphere (UTLS, 200-400hPa), ERA5 RH values remain higher than radiosondes, with or without GRUAN reprocessing. In UTLS (200-200hPa), we have a difference of 6-16% between ERA5 and GRUAN compared to 12-19% between ERA5 and METEO-FRANCE. This confirms partially Dupont et al., (2020) who showed that the GRUAN correction reduces the uncertainties of the M10 technique by 4% at all altitudes during the day and at night.

This project has received funding from the European Union's Horizon Europe Research and innovation program under Grant Agreement No 101056885

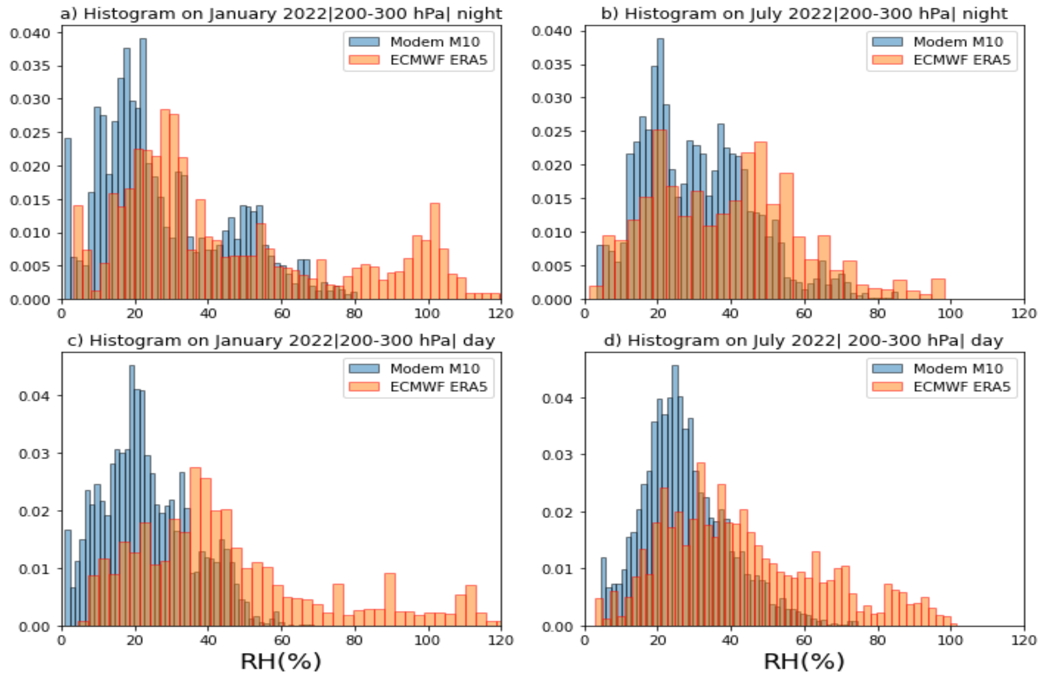

Figure 14 Relative humidity distribution values between 200 and 300 hPa during the night in january 2022 (a) and july 2022 (b), and during the day in January 2022 (c) and july 2022 (d)

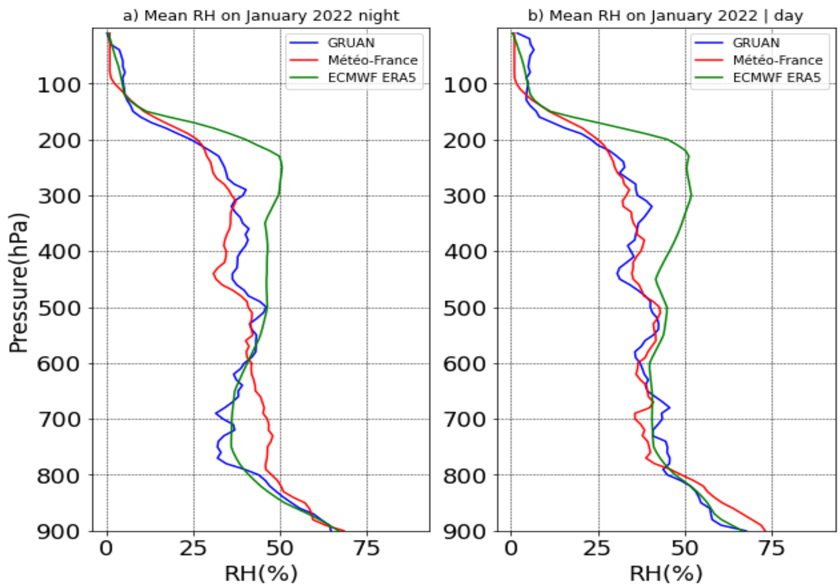

Figure 15 Vertical Relative humidity profiles reprocessed with GRUAN correction (blue), Meteo-France operationnal data processing (red) and ECMWF ERA5 (green) in January during the night (a) and day (b).

This project has received funding from the European Union's Horizon Europe Research and innovation program under Grant Agreement No 101056885

4.3. Conclusions and perspectives

In this study, we presented monthly mean comparisons of relative humidity between ERA5 reanalysis and M10 radiosondes performed at Nimes (France). In the UTLS region (200-300 hPa), higher relative humidity is observed in the ERA5 analyzes compared to radiosondes. The differences are 22% during the day and to 11% at night, 21% in winter and 15% in summer. We showed that the corrections proposed by [Dupont et al., 2020] on the M10 technique could reduce these biases by 7% in 900-500ha and 3-6% in 200-300hPa. In the future, the comparison can be extended by including the Vaisala radiosondes available in the GRUAN network (RS92 or RS41 probes) and the new MODEM M20 probes deployed in Météo-France stations since the beginning of 2023.

5. General Conclusion

The deployment of lidar systems across the four designated sites marks a significant milestone in our project. The successful reactivation of all four systems, coupled with the upgrades of the Observatory's system (OHP) to incorporate a coaxial setup similar to that of La Réunion, enhances our observational capabilities. Leveraging the geographical positioning and performance capacities of the OHP and SIRTA systems, we aim to assess the humidity conditions conducive to contrail formation. Meanwhile, the OPAR (La Réunion) system will complement validation efforts for meteorological analyses, radiosonde data, and potentially satellite observations in the lower stratosphere.

A standardized analysis code for processing lidar water vapor observations, incorporating a unified calibration approach, has been developed. Utilizing ERA5 meteorological analyses, readily available across all sites on an hourly basis, calibration efforts focus on the 3-5 km altitude range, anchored by known-quality radiosonde data. Hourly calibration is subsequently evaluated over longer periods, with post-adjustments made to calibration coefficients to ensure temporal stability.

Comparative analyses between radiosonde data and meteorological analyses have revealed a commendable agreement in the 3-7 km altitude range. However, systematic discrepancies emerge in the upper troposphere, a critical region for contrail formation, indicating potential biases, likely attributable to radiosonde time response issues. Proposed corrections aim to reconcile these differences, striving for alignment between radiosonde data and ERA5 analyses in this altitude domain. Initial lidar observations corroborate these findings, suggesting that biases originate from sondes while hinting at potential underestimations of water vapor content in ERA5 compared to lidar observations.

The regular dispatch of M10 radiosondes from the lidar sites has enriched our dataset with humidity data, facilitating a comprehensive evaluation of simulated humidity levels by the European Centre for Medium-Range Weather Forecasts (ECMWF) through the ERA5 analysis product. This evaluation has led to proposed adjustments in the upper troposphere between ERA5 and Modem sondes, refining our understanding of atmospheric moisture dynamics.

In essence, the culmination of these efforts underscores the importance of integrated observational approaches and meticulous calibration strategies in advancing our understanding of atmospheric dynamics, particularly in the context of contrail formation. Moving forward, ongoing studies within the project framework will delve deeper into these findings, driving continuous refinement and validation of our methodologies and lay the groundwork for further exploration within the project's subsequent phases.

This project has received funding from the European Union's Horizon Europe
Research and innovation program under Grant Agreement No 101056885

Better Contrails Mitigation - BeCoM

Milestone 3
Lidar Software

Delivery Date:	18/08/23
Date of submission:	08/04/24

LEAD BENEFICIARY FOR THIS DELIVERABLE			
Name:	5-CNRS		
Contact Person:			
E-mail:	dunya.alraddawi@latmos.ipsl.fr		
AUTHORS			
Participants:	CNRS		
Work Package:	1		
Version:	1	Number of Pages:	

REVISION HISTORY			
VERSION	DATE	AUTHOR / REVIEWER	NOTES
1	22/03/24	Dunya Alraddawi	

REVIEWED AND SIGNED OFF BY			
ROLE	DATE	NAME	SIGNATURE

This project has received funding from the European Union's Horizon Europe Research and innovation program under Grant Agreement No 101056885

Abstract

Investigation of contrail formation has reactivated the requirement of accurate water vapor in the upper troposphere at cruise altitude. The French community has developed 4 Raman lidars with these capabilities from mid-latitude to tropics. Water vapor mixing ratio is proportional to the ratio of H2O and N2 Raman signals for the same altitude, so a calibration process is needed to give a physical meaning to this ratio. While for coaxial systems a calibration with independent measurement of the water vapor total column is pertinent, another method is required for non-coaxial systems. A more universal external calibration method is adopted, using co-located ERA-5 hourly water vapor profiles that assimilate radiosondes in the lower troposphere.

This milestone describes the united lidar software of the 4 lidar systems, we start by the the uncalibrated WVMR treatment algorithme, then the error estimation and we end by the method to get the calibrated WVMR.

This project has received funding from the European Union's Horizon Europe
Research and innovation program under Grant Agreement No 101056885

List of abbreviations

WVMR	Water Vapor Mixing Ratio
SNR	Signal to Noise Ratio
ECMWF	European Centre for Medium-range Weather Forecasts
GRUAN	GCOS Reference Upper-Air Network
IPRAL	*IPSL* Hi-Performance multi-wavelength Raman *Lidar*
NDACC	Network for Detection of Atmospheric Composition Changes
OHP	Observatory of Haute-Provence
OPAR	Observatoire de Physique de l'Atmosphère de La Réunion
CFH	Cryogenic Frost Point Hygrometer
GNSS	Global Navigation Satellite System
IWV	Integrated Water Vapor
FTIR	Fourrier Transform Infrared Spectroscopy

This project has received funding from the European Union's Horizon Europe Research and innovation program under Grant Agreement No 101056885

List of figures

This project has received funding from the European Union's Horizon Europe Research and innovation program under Grant Agreement No 101056885

Table of content

This project has received funding from the European Union's Horizon Europe Research and innovation program under Grant Agreement No 101056885

1. Introduction

The water vapor profile was defined as one target component of the NDACC (Network for Detection of Atmospheric Composition Changes). The NDACC lidar group selected Raman method for water vapor and exchanges experiences between groups to achieve such a challenge.

The Raman lidar technique is a refinement of the lidar method that permits the profiling of the water vapor mixing ratio with high resolution and accuracy. These informations can be used to better understand the humidity conditions accompanying the contrails construction process and persistence.

Using a standard high-power laser useful information can be extracted from some portion of the spectrum of the atmospheric backscattered signal.

Water vapor information can be derived from the Raman lidar backscatters in photon counting system (PCS) as described by Sherlock et al. (1999a), Hoareau et al. (2009), received at specific wavelengths corresponding to water vapor and nitrogen molecules during nightly seances in the absence of low clouds.

Lidar water vapor measurements have also some limitations, as it probes the atmosphere to get a humidity content that gets smaller with altitude until a very sensitive variability around the tropopause. Hence, a careful calibration is needed, using co-located external vertical profile measurements from Radiosondes, CFH sondes, models etc, or even total integrated humidity content as from GNSS.

One of the main challenges of the current treatment is the choice of improved Calibration method and to carefully consider the calibration uncertainty, to be adapted in order to unify the treatment protocole over multi lidar sites on the French territory, in spite of different acquisition modes and telescope FOV over these sites. Hereafter a bref description of the treatment method and the suggested calibration strategy is given.

2. Water Vapor Mixing Ratio « WVMR » Equation

Raman measurements are performed with the ratio of the Raman water vapor channel and the Nitrogen Raman Channel (Sherlock et al.,1999a). Then a direct measurement of the water vapor mixing ratio is obtained.

In order to get water vapor mixing ratio profile, Raman backscattered signals returned respectively at 607 (or 387) nm by Nitrogen and at 660 (or 408) nm by atmospheric water vapor are used, corrected for background noise, accounting for the atmospheric differential transmission T(z) and scaled by the calibration coefficient C (to be detailed later). Signals are measured by number of photons/bin/shot as following:

$$WVMR(z) = C \cdot T(z) \cdot \frac{S_{\mathrm{H_2O}}(z) - B_{\mathrm{H_2O}}(z)}{S_{\mathrm{N_2}}(z) - B_{\mathrm{N_2}}(z)}$$

Where :

C : The Calibration factor

$T(z)$: The atmospheric differential transmission

$S_{\mathrm{H_2O}}(z)$: H_2O Raman signal

$B_{\mathrm{H_2O}}(z)$: H_2O Raman Background signal noise

$S_{\mathrm{N_2}}(z)$: N_2 Raman signal

This project has received funding from the European Union's Horizon Europe Research and innovation program under Grant Agreement No 101056885

$B_{N_2}(z)$: N_2 Raman Background signal noise

$S_{H_2O}(z) - B_{H_2O}(z)$: H_2O Cleaned signal

$S_{N_2}(z) - B_{N_2}(z)$: N_2 Cleaned signal

It has been shown that the relative transmission of the Raman returns due to the cirrus clouds is negligibly small for altitudes above 4 km. Consequently, no attenuation corrections have been applied (Sherlock et al. 1999a) .

3. Lidar Traitement Channel

3.1. Optical and periodic Integrations

The statistical nature of the incoherent laser soundings requires (for a given altitude) raw data being integrated over a number of laser successive shots and hence improve the signal to noise ratio SNR. More simply, each integration period consists of the photon counts of certain number of shots (8000 for OHP) for each altitude bin of few meters (75m for OHP, 15m for IPRAL, and so on), these counts constitute a signal profile with altitude.

Previous studies (Hoareau et al. 2009, Dionisi et al.2015) have determined the least total integration period as about 27 minutes of consecutive measurements, This should allow to consider the air masse stability and describe a vertical water vapor profile. The current treatment will be based on hourly screening to get a vertical profile that might reach an altitude of 12 km, longer periods might result in a several atmospheric situations mixed-up unrealistic profile. This hourly profile choice enable the calibration and avoid to lost interesting information about the variability of the local concentration. In some cases, another pre-filtering is applied to get only night measurements if the system operates with a day/night continuous rythme (like for IPRAL).

3.2. Noise correction

Atmospheric signals, particularly H_2O and N_2 ones exhibit inherent noise, that can obscure valuable information, accurate estimation of this noise is essential. Skylight background noise B_x is due to skylight brightness, thermal noise of the multiplier and signal-induced noise of a large initial burst.

The statistical distribution of photon pulses is expected to follow the « Poisson distribution », Note that Water vapor Raman signals are two order of magnitude smaller than Nitrogen Raman signals. However Noise magnitude is not likely to follow the same logic, see figure 1.

Historical Lidar SNR analysis for the period between 2001-2010 show that most signal above 20 km from H_2O wavelengths and above 50 km for N_2 wavelengths are assumed to primarily comprise noise.

Hence, The background noise model is estimated as the median of the photon counts (signal) for altitudes > 20 km for H_2O signal noise, and > 50 km for N_2 one.

The error associated with noise calculation is estimated using statistical bootstrapping, a specific number of bootstrapped iterations (default: 1000) are performed to generate resampled datasets, from which bootstrapped medians are computed, the standard deviation of the bootstrapped medians provides an estimate of the error in the noise calculation.

This project has received funding from the European Union's Horizon Europe Research and innovation program under Grant Agreement No 101056885

3.3. Signal Cleaning

Lidar raw signals have to be smoothed to enhance their quality. An adaptive Blackman window filtering is tailored to accommodate varying altitudes and signal characteristics. Filter window sizes are adjusted based on altitude while a decay factor is incorporated beyond specified altitude limits according to the signal magnitude. The vertical resolution remained unchanged.

Cleaned signal is the lidar signal resulting after signal smoothing and noise removing process, the signal cleaning is assuring that only relevant signal components are retained. Subsequently, the cleaned signal undergoes interpolation to handle zero or negative values (altitudes of SNR <=1), such outlier values are replaced with interpolated values from neighboring positive data points and decaying towards zeros.

See figure 1 for an example of the raw and cleaned Raman signals of a full night integrated measurements and their noise level. Water vapor signal is shown to extend up to 11 km for this exemple. While nitrogen signal is detectable up to about 43 km.

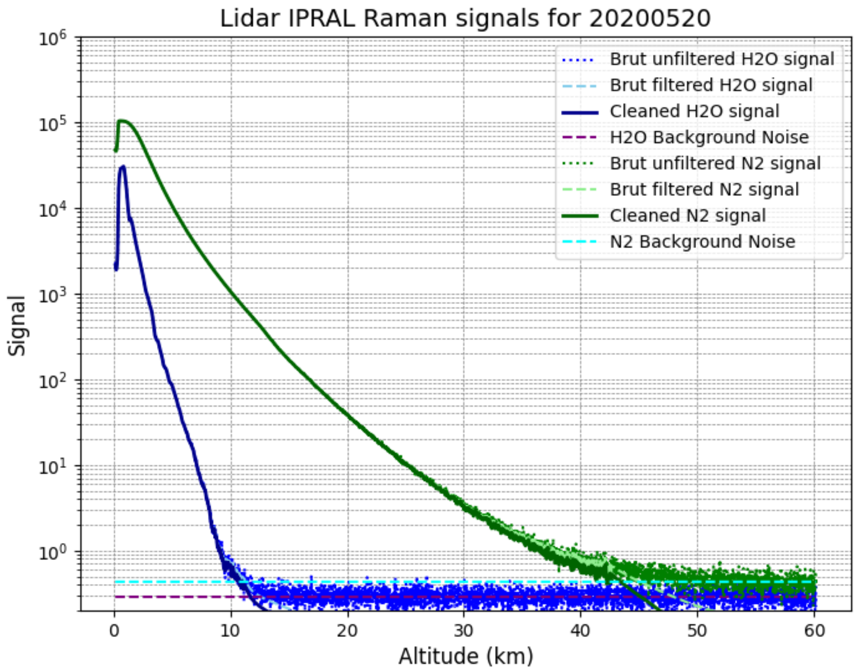

Figure 1. Example of Raman lidar signals: Brut, filtered, cleaned with the associated noises, Blues for H2O , and greens for N2 .

4. WVMR Error estimation

Most of the lidar methods are based on a ratio of two simultaneous signals, and thus immune to long term instrumental drift and measurement conditions. Systematic errors are expected to be reduced by hard-ware design, Thus, the signal processing related to measurement uncertainties is based on random errors (Sherlock et al.1999). The two principal error sources considered here are

This project has received funding from the European Union's Horizon Europe Research and innovation program under Grant Agreement No 101056885

photon counting and skylight background estimation, one evident extra error source will be related to the calibration factor estimation.

4.1. Signal Detection Error

The signal detection error (also referred to as photon-counting error) process is described by Poisson statistics, and the standard deviation of the measurement is $\sigma = \sqrt{N}$, where N is the number of photons counted. This error represents the uncertainty in determining the WVMR due to inherent variations and noise in the lidar signals. It is estimated based on the cleaned signals of H_2O and N_2, along with the brut signals respective detection errors. The detection error is calculated as the root mean square (RMS) of the relative errors associated with H_2O and N_2 signals, adjusted by their respective noise levels. This provides a comprehensive assessment of the detection error in the WVMR estimation process as following:

$$WVMR_{\text{detection\_err}} = \sqrt{\left(\frac{1}{\left(S_{\mathrm{N_2}}(z) - B_{\mathrm{N_2}}(z)\right)} \cdot S_{\mathrm{H_2O,err}}(z)\right)^2 + \left(\frac{S_{\mathrm{H_2O}}(z) - B_{\mathrm{H_2O}}(z)}{\left(S_{\mathrm{N_2}}(z) - B_{\mathrm{N_2}}(z)\right)^2} \cdot S_{\mathrm{N_2,err}}(z)\right)^2}$$

Where :

$S_{\mathrm{N_2}}(z)$: N_2 Raman signal

$B_{\mathrm{N_2}}(z)$: N_2 Raman Background signal noise

$S_{\mathrm{N_2}}(z) - B_{\mathrm{N_2}}(z)$: N_2 Cleaned signal

$S_{\mathrm{H_2O,err}}(z)$: H_2O Raman brut signal detection error

$S_{\mathrm{N_2,err}}(z)$: N_2 Raman brut signal detection error

$S_{\mathrm{H_2O}}(z) - B_{\mathrm{H_2O}}(z)$: H_2O Cleaned signal

4.2. Noise Detection Error

Similar to the detection error, the noise estimation error is calculated using RMS of the relative errors, reflecting the combined impact of noise estimation inaccuracies on WVMR calculations. The noise estimation error is computed using the following equation:

$$WVMR_{\text{noise\_err}} = \sqrt{\left(\frac{1}{\left(S_{\mathrm{N_2}}(z) - B_{\mathrm{N_2}}(z)\right)} \cdot B_{\mathrm{H_2O,err}}(z)\right)^2 + \left(\frac{S_{\mathrm{H_2O}}(z) - B_{\mathrm{H_2O}}(z)}{\left(S_{\mathrm{N_2}}(z) - B_{\mathrm{N_2}}(z)\right)^2} \cdot B_{\mathrm{N_2,err}}(z)\right)^2}$$

Where :

$S_{\mathrm{N_2}}(z)$: N_2 Raman signal

$B_{\mathrm{N_2}}(z)$: N_2 Raman Background signal noise

This project has received funding from the European Union's Horizon Europe Research and innovation program under Grant Agreement No 101056885

$S_{N_2}(z) - B_{N_2}(z)$: N_2 Cleaned signal

$B_{H_2O,err}(z)$: H_2O Background noise estimation error

$B_{N_2,err}(z)$: N_2 Background noise estimation error

$S_{H_2O}(z) - B_{H_2O}(z)$: H_2O Cleaned signal

4.3. Calibration Error

This error is the RMSE between the Calibrated Lidar profile and the referenced profile for calibration, taking into account both profile portions between 3 and 5 km of altitude (calibration zone).

4.4. WVMR total Error

The total WVMR error is calculated for certain period (hour or even full night), taking into account 3 sources of uncertainty and variability in the measurements:

I. **Calibrated Detection Error**: The detection error (section 4.2), representing the uncertainty in detecting and quantifying the WVMR signal, is calibrated to reflect the scaling factors for this hour (or night).

Calibrated Detection Error = $WVMR_{\text{detection\_err}}/Calibration_{\text{factor}}$

II. **Calibrated Noise Error**: The noise estimation error (section 4.3) is first calibrated to account for any scaling factors. This calibration process adjusts the noise error for the hour (or night) based on the corresponding calibration factor.

Calibrated Noise Error = $WVMR_{\text{noise\_err}}/Calibration_{\text{factor}}$

III. **Calibration Error**: The error introduced during the calibration process itself is considered. This error accounts for any discrepancies or inaccuracies in the calibration procedure, impacting the final WVMR estimation.

Calibration error = $WVMR_{\text{Calibration\_err}} * WVMR$

The total WVMR error is the sum of the previous three errors, see figure 2.

$$WVMR_{\text{Total\_err}} = WVMR_{\text{detection\_err}}/Calibration_{\text{factor}} + WVMR_{\text{noise\_err}}/Calibration_{\text{factor}} + WVMR_{\text{Calibration\_err}} * WVMR$$

5. Lidar Calibration

Water vapor mixing ratio as a physical parameter is proportional to the ratio of the H_2O and N_2 Raman channels signals. The calibration process is conducted to give a geophysical meaning of this ratio to be converted on a real WVMR profile by a scale factor. The application of lidar measurements to climatological study requires a robust calibration of the instrument. Different calibration methodologies have been developed (Whiteman et al., 2006; Leblanc et al., 2012; Hoareau et al., 2009; Dionisi et al., 2010; Bock et al., 2013). Two principal ways are known to calculate this conversion factor (calibration factor):

- Internal method: this method consists of calculating/measuring each term composing the calibration constant, each representing a source of incertitude relevant parameters of the lidar system (ex: temperature dependance of the Raman cross-section) to be measured or calculated experimentally using standard laboratory procedures (Sherlock et al.,1999,

This project has received funding from the European Union's Horizon Europe Research and innovation program under Grant Agreement No 101056885

Venable et al.,2011). This method presents larger margins of errors accumulated, and thus less recommended when accurate measurements are requested.

- External method: this method estimates the total calibration coefficient as the ratio between a reference instrument, and the uncalibrated lidar data and the calibration therefore depends on the accuracy of another instrument that also presents its own limitations.
    - Co-axial systems : Calibration using a referenced TCWV quantities, as for OPAR (La réunion island - France (Hoareau et al.,2012; Dionisi et al.,2015; Vérèmes et al.,2019). GNSS integrated water vapor quantity is used to get the calibration factor (the coincident integrated water vapor lidar quantity is calculated and the ratio of both quantities for certain period is considered as the scale factor of the period).
    - Bi-axial systems : Calibration using referenced WVMR profil, as for OHP and IPRAL lidars. Since the lidar profile is not extended to sol, the reference need to provide a vertical WVMR profile, to enable a comparaison for certain zone of the profile and hence calibrate the full profile. This method can also be applied to calibrate co-axial lidars, so it is chosen to unify the calibration strategy over the four lidars on the French territories.

5.1. Reference choice

Many techniques are capable to provide WVMR referenced profiles for lidar calibration, like Radiosondes, laser Diodes, CFH, balloon-borne frost-point Hygrometers, or FTIR measurements on meteorological stations (Bock et al., 2013, Dionisi et al.,2015, Leblanc et al.,2012, Vowel et al.,2007, Meyer et al.,2015). These instruments have their potentials as references to describe WVMR in the troposphere but they have also their limitations. Starting from expensive long-term operational cost, and passing by limited accuracy on upper troposphere, it’s very complicated to find the suitable instrument for a long term calibration strategy.

The French sites are supplied with radiosondes measurements twice a day (midnight and midday lunchs) which provide a well qualified data set but found to have a serious limitation of discontinuities at individual stations (humidity sensor response, material change, etc.) and a poor sensitivity in the upper troposphere due to the radiosonde derivation from the zenith above the site by wind. Also, radiosondes don’t give a sufficient temporal coverage to calibrate a short time WVMR profile (hourly fro exemple) and detect thereby an interesting events on the above site air-masse, hence hourly calibration references profiles are needed.

The ECMWF latest hourly re-analyses datasets named ERA-5 (Hersbach et al.,2023), represents the fifth generation of the European Centre for Medium-Range Weather Forecasts – ECMWF reanalysis, providing a comprehensive overview of global climate and weather spanning the past eight decades. Data is accessible from 1940 onwards, marking a transition from the previous ERA-Interim reanalysis. Gridded data provided by ERA5 have a horizontal resolution of 0.25° x 0.25°. It provides vertical coverage between 1000 hPa to 1 hPa, with a vertical resolution of 37 pressure levels, and hourly temporal resolution (Hersbach et al., 2023).

Forced by radiosondes, ERA-5 shows a good quality to make climatological studies, but are suspected to miss local short term events too. Trying to assess the limitations of these re-analyses with respect to the radiosondes, the results show a dry radiosonde bias that gets more important with altitude, the best agreement being found on altitudes between 3 and 5 km see Figure 2.

This project has received funding from the European Union’s Horizon Europe Research and innovation program under Grant Agreement No 101056885

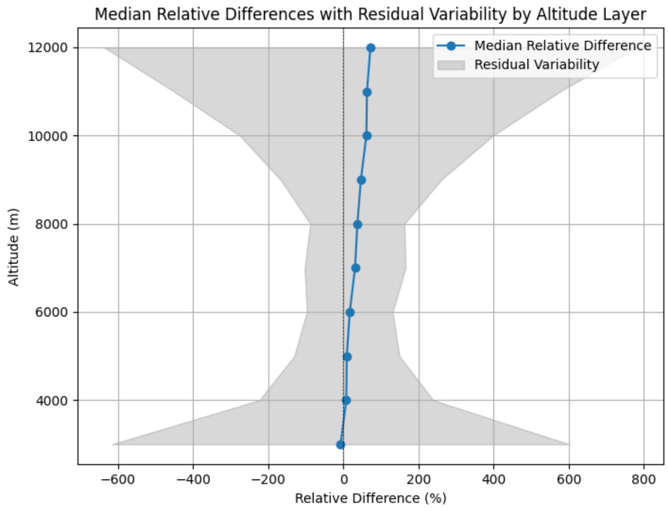

Figure 2. Relative Error (ERA-5 ,MF-Radiosonde) of Relative humidity profiles cases coincident to lidar measurements (OHP: 2001-2010) and the residual variability.

5.2 Calibration Method

Collocated and simultaneous Lidar water vapor mixing ratio (WVMR) hourly profiles (Level 2) from cleaned signals (Level 1)are calibrated using hourly ERA-5 reanalysis data, between 3 & 5 km. The collocated 37 pressure levels reference is considered allowing a maximal spatial drift of 0.1° and the best temporal coincident (same lidar measurements dominant hour). The Extern calibration strategy undergoes the following steps:

Altitude Range Selection: The calibration process focuses on a specific altitude range, typically between 3 to 5 kilometers above ground level (km). This range is chosen to ensure that calibration factors are derived from regions of the atmosphere where both lidar and ERA5 hourly data exhibit reliable measurements.

Data Preparation: The ERA-5 profiles are prepared by reversing their altitude arrays to match the ascending altitude sequence of the lidar instrument. The ERA5 profile within the calibration range is interpolated onto the lidar altitude grid. Altitude and profile data within the selected calibration range are extracted from both datasets for further processing.

Calibration Factors Calculation: Calibration factors are then calculated by dividing the lidar WVMR profiles by the interpolated ERA5 profiles. These calibration factors represent the scaling factors required to align the lidar measurements with the ERA5 reference data within the selected altitude range.

Hourly Profile Calibration: The entire lidar altitude profile calibration is obtained as the mean of the calibration factors of the selected altitude range. This process ensures that the entire lidar profile is calibrated consistently with one hourly calibration factor.

Error and uncertainties Estimation: The calibration process includes the estimation of calibration errors to quantify the discrepancies between the calibrated lidar profiles and the ERA5 reference data. Root Mean Squared Error (RMSE) and correlation coefficient metrics are calculated to assess the accuracy and reliability of the calibration process.

Full night Calibration & validation: Hourly Calibration factors which are issues of significantly correlated hourly WVMR lidar profiles lidar to ERA-5 ones between 3 & 5 km, are averaged each night of measurement and are named nightly coefficient. Nightly calibrated profiles are validated against colocated radiosondes ones when possible, I.e corrected radiosondes dataset (Dupont et al.,2020).

This project has received funding from the European Union’s Horizon Europe
Research and innovation program under Grant Agreement No 101056885

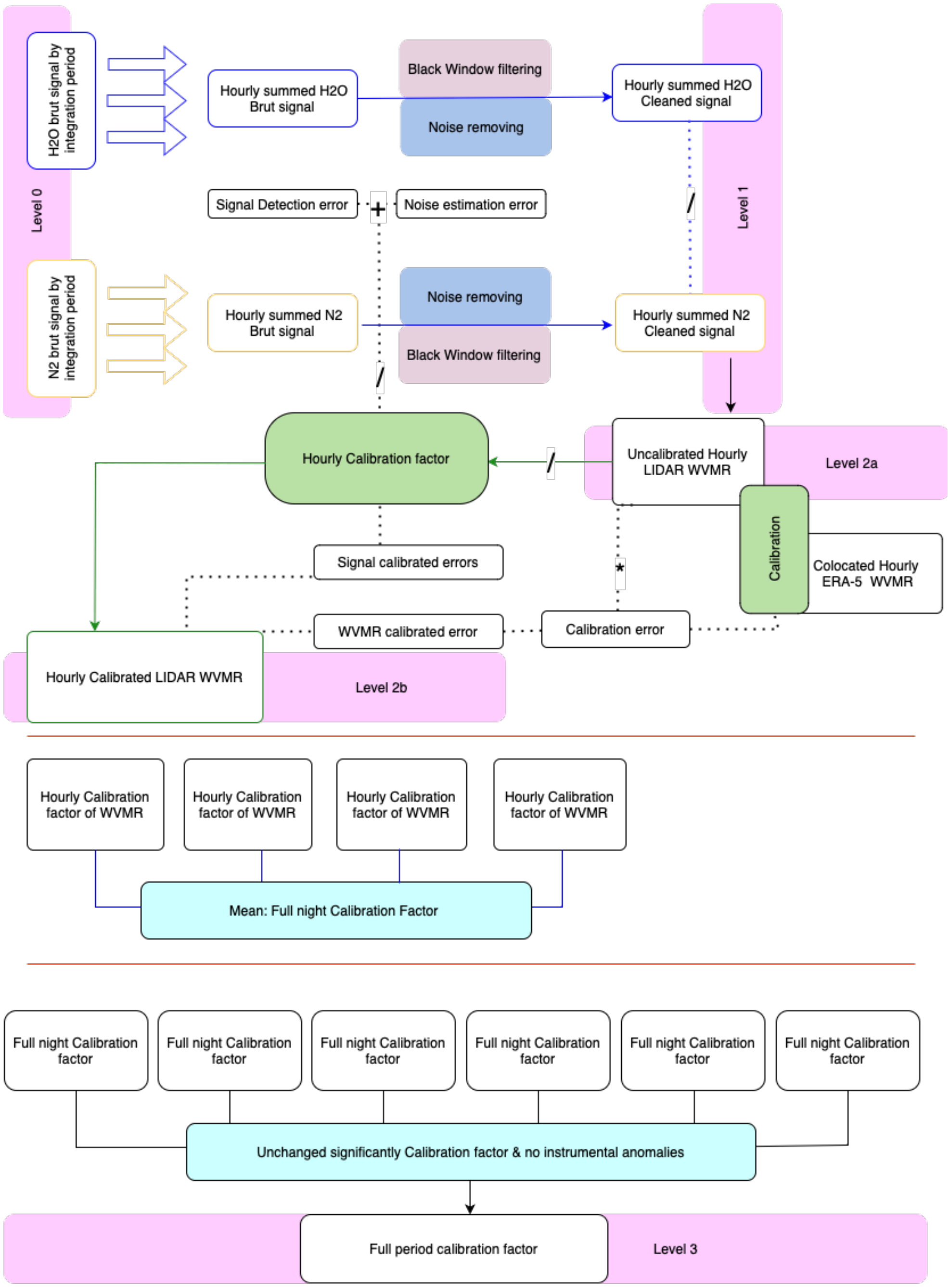

Figure3. Diagram of Raman Lidar Treatment channel using Externe Calibration Strategy via ERA-5 Hourly profiles.

Full period Calibration & validation: The evolution of the calibration coefficient over a long enough period permits one to adjust the series to instrumental changes that are unavoidable in a long commitment (ageing and/or substitution of filters, fiber- optic, receiving optic alignment, detectors, etc.). The average nightly coefficient between two instrumental changes detected is considered as the “calibration coefficient” of each measurement performed during this period.

Figure 3 describes the treatment channel from the shortest integrated Raman signals (Level 0 or Brut data) to the calibrated full period WVMR profiles (Level 3: full nights profiles calibrated with the same calibration factor as belongs to a stationary period: archived data), passing by the hourly

This project has received funding from the European Union’s Horizon Europe Research and innovation program under Grant Agreement No 101056885

summed cleaned data (level 1) and quasi-real time uncalibrated hourly WVMR (level 2a), and the hourly calibrated ones(Level2b).

While Figure 4a illustrates two exemples of WVMR profiles obtained from lidar measurements at OHP (left) and at SIRTA (right), where radiosondes (Meteo-France M10) WVMR profiles (black) show a clear wet bias compared to colocated ERA-5 re-analysis profile (magenta) used for calibration of Lidar uncalibrated profile (red), and thereby with respect to the calibrated lidar profile (green) presented also along with the associated errors (green shadows).

The upper panel of figure 4a depicts one-hour (midnight) Water Vapor Mixing Ratio (WVMR) profiles acquired from lidar measurements, along with the calibration references ERA-5 and the nearest collocated Meteo-France (M10) Radiosonde profile for the midnight hour for validation purposes. The panel is zoomed to provide a detailed view of the lower profile portion between 3 and 5 km altitude, which serves as the calibration range. Lidar profiles are significantly correlated (80%) to radiosondes on the calibration range (3-5 km), and best to ERA-5(around 99%)..

The middle panel extends the analysis to show WVMR profiles up to 10 km altitude for the same hour. Uncalibrated & calibrated lidar, ERA-5, and Radiosonde profiles are presented, offering a comprehensive view of the atmospheric water vapor distribution over an extended altitude range. Hourly calibrated lidar profiles (up to 12 km) are significantly correlated to the collocated radiosonde ones by 65% and 70% at SIRTA (IPRAL) and OHP respectively. A much better correlation to ERA-5 is noted (better than 90% on both sites).

The bottom panel provides a holistic view of the full-night calibrated WVMR profiles, capturing the variations in water vapor content throughout the night (3,6 hours integrated at IPRAl, OHP respectively). The inclusion of collocated radiosonde data (midnight) facilitates validation of the calibrated lidar measurements. The added ERA-5 profile is that of the mid-night hour (coinciding with radiosonde one).

Figure 4b illustrates two other examples of WVMR profiles obtained from other dates lidar measurements at OHP (left) and at SIRTA (right), where radiosondes (Meteo-France M10) WVMR profiles (black) show this time a clear dry bias (as expected from previous studies and most case studies, So that smaller RS magnitudes are observed compared to collocated ERA-5 re-analysis profile (magenta) used for calibration of Lidar uncalibrated profile (red), and thereby with respect to the calibrated lidar profile (green) presented also along with the associated errors (green shadows).

The three panels have similar signification as those of figure 4a, with zoomed hourly WVMR profiles obtained between 3 and 5 km height for all three instruments in the upper panel, and an extended view of the WVMR profiles up to 10 km on the middle panel, and the full night integrated lidar profile (6 hours integrated at each of IPRAl, OHP , total period centered at mid-night) presented with the mid-night colocated radiosonde and the coincident (to Radiosonde) ERA-5 hourly profile.

The overall agreement between radiosonde, ERA-5 and full night lidar profiles(Figure 4b), as well as the vertical variability in water vapor content within the atmosphere by the different techniques is figured out. Lidar and Radiosondes profiles up to 12 km are significantly correlated at 70% (OHP) and at 74% (SIRTA). Lidar and ERA-5 profiles are significantly correlated (more than 90% on both sites).

This project has received funding from the European Union's Horizon Europe Research and innovation program under Grant Agreement No 101056885

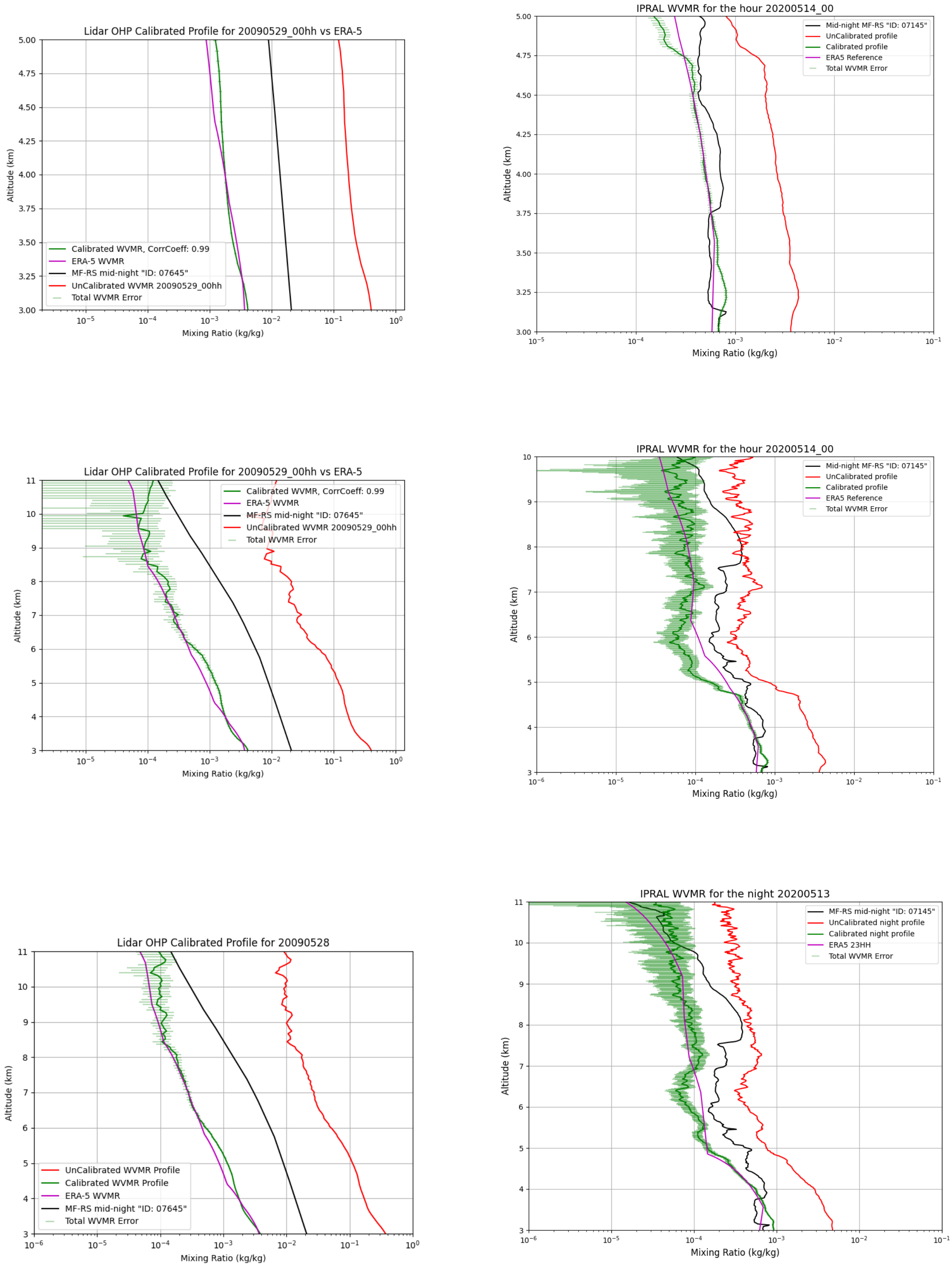

Figure 4a. Exemple of drier (than RS) Raman Lidar full night WVMR profile. Left for OHP, Right for IPRAL lidar calibrated using Externe Calibration Strategy via ERA-5 Hourly profiles. Upper figure: midnight hourly calibration profiles between 3 & 5 km, middle figure: same hour extended profile up to 10 km, bottom: full night calibrated profile. Legends: In red is the uncalibrated lidar profile, in green the calibrated one, in black the colocated Meteo-France (M10) radiosonde mid-night WVMR profile, in magenta the hourly ERA-5 colocated calibration reference, total WVMR errors are represented in green shadows.

This project has received funding from the European Union's Horizon Europe Research and innovation program under Grant Agreement No 101056885

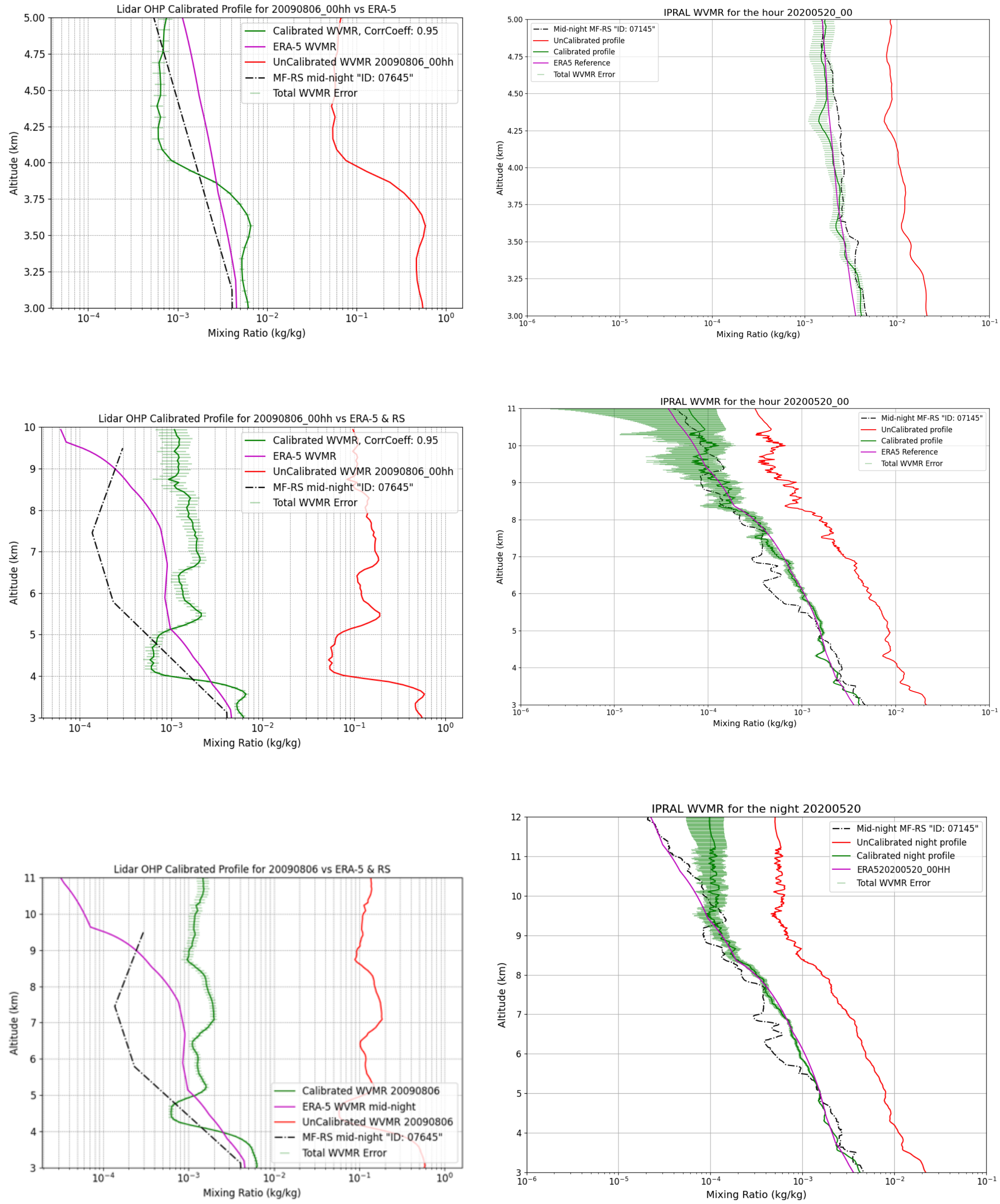

Figure 4b. Exemple of more humide (than RS) Raman Lidar full night WVMR profile. Left for OHP, Right for IPRAL lidar calibrated using Externe Calibration Strategy via ERA-5 Hourly profiles. Upper figure: midnight hourly calibration profiles between 3 & 5 km, middle figure: same hour extended profile up to 10 km, bottom: full night calibrated profile. Legends: In red is the uncalibrated lidar profile, in green the calibrated one, in black the colocated Meteo-France (M10) radiosonde mid-night WVMR profile, in magenta the hourly ERA-5 colocated calibration reference, total WVMR errors are represented in green shadows.

This project has received funding from the European Union's Horizon Europe Research and innovation program under Grant Agreement No 101056885

Overall, some other investigations on calibration methods including collocated radiosonde are under investigation, to be compared with our method. This new developed software provides valuable information about the humidity content in the 7-11 km range, altitudes of a possible contrail formation, and will be used to force models and to better understand contrails formation and persistence. This software is part of European project BeCom, allowing a better view of the potential contribution of contrail in future air traffic regulation.

6. Conclusion

This milestone describes the universal calibration approach to be adopted, leveraging co-located ERA-5 hourly water vapor profiles assimilating radiosonde data from the lower troposphere. Hourly integration periods of lidar water vapor mixing ratio (WVMR) are compared with corresponding ERA-5 re-analyses, with hourly calibration factors from which nightly calibration factors are derived. Daily calibrations are scrutinized to identify any instrumental effects on calibration coefficients, with final coefficients calculated for quasi-stationary periods. Additionally, at certain sites, collocated radiosondes observations are examined and compared with ours.

In conclusion, the methodology presented herein exhibits versatility, applicable across diverse sites, although its ultimate refinement requires a comprehensive dataset for calibration. Encouragingly, our results exhibit a robust agreement with both ERA5 reanalysis and Metro France Modem 10 radiosonde observations within the lower troposphere (3-7 km), thereby validating its efficacy in this altitude regime. However, preliminary analyses suggest a potential underestimation of water vapor by ERA5 at higher altitudes (>10 km), necessitating deeper uncertainty assessment, is conducted in section 4. Further investigation and refinement in subsequent project phases.

The newly developed software enables valuable insights into humidity content within the 7-11 km range, crucial altitudes for potential contrail formation. This software will advance our comprehension of contrail formation and persistence dynamics, and the potential impact of contrails on future air traffic regulation.

7. References

Bock, O., Bosser, P., Bourcy, T., David, L., Goutail, F., Hoareau, C., Keckhut, P., Legain, D., Pazmino, A., Pelon, J., Pipis, K., Poujol, G., Sarkissian, A., Thom, C., Tournois, G., and Tzanos, D.: Accuracy assessment of water vapour measurements from in situ and remote sensing techniques during the DEMEVAP 2011 campaign at OHP, Atmos. Meas. Tech., 6, 2777–2802, 2013..〈10.5194/amt-6-2777-2013〉

Dionisi, D., F. Congeduti, G. L. Liberti, and F. Cardillo, 2010: Calibration of a Multichannel Water Vapor Raman Lidar through Noncollocated Operational Soundings: Optimization and Characterization of Accuracy and Variability. J. Atmos. Oceanic Technol., 27, 108–121,2010 〈10.1175/2009JTECHA1327.1〉

Dionisi, D., Keckhut, P., Courcoux, Y., Hauchecorne, A., Porteneuve, J., Baray, J. L., Leclair de Bellevue, J., Vérèmes, H., Gabarrot, F., Payen, G., Decoupes, R., and Cammas, J. P., Water vapor observations up to the lower stratosphere through the Raman lidar during the Maïdo lidar calibration campaign, Atmos. Meas. Tech., 8, 1425-1445.〈10.5194/amt-8-1425-2015〉

Dupont, J., M. Haeffelin, J. Badosa, G. Clain, C. Raux, and D. Vignelles, 2020: Characterization and Corrections of Relative Humidity Measurement from Meteomodem M10 Radiosondes at Midlatitude Stations. *J. Atmos. Oceanic Technol.*, **37**, 857–871, 〈10.1175/JTECH-D-18-0205.1〉.

This project has received funding from the European Union's Horizon Europe Research and innovation program under Grant Agreement No 101056885

Hersbach, H., Bell, B., Berrisford, P., Biavati, G., Horányi, A., Muñoz Sabater, J., Nicolas, J., Peubey, C., Radu, R., Rozum, I., Schepers, D., Simmons, A., Soci, C., Dee, D., Thépaut, J-N. (2023): ERA5 hourly data on pressure levels from 1940 to present. Copernicus Climate Change Service (C3S) Climate Data Store (CDS), (Accessed on DD-MMM-YYYY). 〈 10.24381/cds.bd0915c6〉

Hoareau, C., P. Keckhut, A. Sarkissian, J-L. Baray, And G. Durry, Methodology for water monitoring in upper troposphere with Raman lidar at observatory of Haute-Provence, Journal of Atmospheric and Oceanic Technology, 26(10), 2149-2160, 2009. 〈10.1175/2009JTECHA1287.1〉

Hoareau, C., P. Keckhut, J.-L. Baray, L. Robert, Y. Courcoux, J. Porteneuve, H. Vömel, and B. Morel, A Raman lidar at la Reunion (20.8° S, 55.5° E) for monitoring water vapor and cirrus distributions in the subtropical upper troposphere: preliminary analyses and description of a future system, Atmos. Meas. Tech., 5(6), 1333-1348, 2012. 〈10.5194/amt-5-1333-2012〉.

Leblanc, T., McDermid, I. S., and Walsh, T. D.: Ground-based water vapor raman lidar measurements up to the upper troposphere and lower stratosphere for long-term monitoring, Atmos. Meas. Tech., 5, 17–36, 2012.〈10.5194/amt-5-17-2012〉

Meyer, J., Rolf, C., Schiller, C., Rohs, S., Spelten, N., Afchine, A., Zöger, M., Sitnikov, N., Thornberry, T. D., Rollins, A. W., Bozóki, Z., Tátrai, D., Ebert, V., Kühnreich, B., Mackrodt, P., Möhler, O., Saathoff, H., Rosenlof, K. H., and Krämer, M.: Two decades of water vapor measurements with the FISH fluorescence hygrometer: a review, Atmos. Chem. Phys., 15, 8521–8538, 2015. 〈10.5194/acp-15-8521-2015〉

Sherlock V., A. Garnier, A. Hauchecorne, and P. Keckhut, Implementation and validation of a Raman lidar measurement of middle and upper tropospheric water vapor, *Applied Optics*, 38, 5838-5850, 1999.〈10.1364/AO.38.005816〉

Venable, D.D.; Whiteman, D.N.; Calhoun, M.N.; Dirisu, A.O.; Connell, R.M.; Landulfo, E. Lamp mapping technique for independent determination of the water vapor mixing ratio calibration factor for a Raman lidar system. *Appl. Opt.* **2011**, *50*, 4622–4632.〈10.1364/AO.50.004622〉

Vérèmes H., Payen G., Keckhut P., Duflot V., Baray J.-L., Cammas J.-P., Evan S., Posny F., Körner S., Bosser P., Validation of the water vapor profiles of the Raman lidar at the Maïdo observatory (Reunion Island) calibrated with global navigation satellite system integrated water vapor, *Atmosphere*, MDPI 2019, 10, pp.713. 〈10.3390/atmos10110713〉.

Vömel, H.; David, D.E.; Smith, K. Accuracy of tropospheric and stratospheric water vapor measurements by the cryogenic frost point hygrometer: Instrumental details and observations. *J. Geophys. Res. Atmos.* **2007**, *112*. 〈10.1029/2007JD008698〉.

Whiteman, D. N., and Coauthors, 2006: Raman water vapor lidar measurements during the International H2O Project. Part I: Instrumentation and analysis techniques. *J. Atmos. Oceanic Technol*, **23 ,** 157–169.〈10.1175/JTECH1838.1〉

This project has received funding from the European Union's Horizon Europe Research and innovation program under Grant Agreement No 101056885